The Rare Disaster Concern Index: RIX*

Weihan Li[†]
Department of Accountancy and Finance
Otago Business School, University of Otago
Dunedin 9054, New Zealand
weihan.li@postgrad.otago.ac.nz

Jin E. Zhang
Department of Accountancy and Finance
Otago Business School, University of Otago
Dunedin 9054, New Zealand
jin.zhang@otago.ac.nz

Xinfeng Ruan
Department of Finance
International Business School Suzhou, Xi'an-Jiaotong Liverpool University
Suzhou 215000, China
edwin.ruan@xjtlu.edu.cn

Pakorn Aschakulporn
Department of Accountancy and Finance
Otago Business School, University of Otago
Dunedin 9054, New Zealand
pakorn.aschakulporn@otago.ac.nz

First Version: 29 Mar 2024
This Version: 1 July 2024

Keywords: Tail Risk, RIX, Third Moment, VIX, SKEW
JEL Classification Code: G12,G13

* Acknowledgements: We are grateful to the stimulating discussions and input received from Tianjiao Li, Wen Xu, and Ruizi Hu during our Derivatives and Quantitative Finance Group meetings. Weihan Li appreciates being awarded the University of Otago Doctoral Scholarship. Jin E. Zhang has been supported by an establishment grant from the University of Otago. Xinfeng Ruan acknowledges financial support from Xi'an Jiaotong-Liverpool University Research Development Fund (project No. RDF-23-01-022) and the Jiangsu Province Distinguished Professor Talent Programme.

[†] Corresponding author.

The Rare Disaster Concern Index: RIX

Abstract

This study aims to deepen the understanding of the Rare Disaster Index (RIX) by redefining its concept, developing its exact model within the Gram-Charlier density, and constructing its time series to enhance its theoretical foundation and numerical application in capturing extreme market risks. Through comparative analysis with conventional indices across various term structures, we uncover the superior capability of the RIX in reflecting higher-order risks in financial markets. Our findings demonstrate the heightened sensitivity of the RIX to extreme market movements, especially within the left lower range, emphasizing its importance in strategic risk management and investment decision-making.

Keywords: Tail Risk, RIX, Third Moment, VIX, SKEW

JEL Classification Code: G12,G13

1 Introduction

In the evolving landscape of financial markets, where the risk of rare but profoundly impactful events poses a major threat, the necessity for robust, predictive measures of tail risk has never been more urgent. The rare disaster index (RIX), first introduced by Du and Kapadia (2012) as a jump and tail index ($JTIX$), stands at the forefront in this field, offering a novel perspective for assessing the dynamics of extreme market volatility. The development of the RIX indicated a critical shift towards identifying and quantifying the vague nature of catastrophic market downturns, which are the events that traditional market volatility indices, such as the Chicago Board Options Exchange (CBOE) Volatility Index (VIX) and Skewness Index ($SKEW$), might not fully encompass. By focusing on the extremities of market behavior, the RIX provides a more detailed view of the potential for substantial losses, making it an important indicator for investors, risk managers, and policymakers alike. The urgency for such a measure has only exacerbated in the wake of recent global financial crises, underscoring the critical need to anticipate and mitigate the threats of these rare but overwhelming disasters.

This study initiates a comprehensive exploration of the RIX, aiming to numerically disclose its characteristics and to underline its significance in indicating the dynamics of market tail risks. Leveraging our enhanced definition of the RIX, this study endeavors to numerically explore the connection between the RIX and higher-order risks, as well as its exact model under the Gram-Charlier density through rigorous mathematical derivations. Moreover, we also estimate the time series of the RIX using the S&P 500 Index options (SPX) to resonate with the practical realities of market dynamics. Through these efforts, we seek to extend the frontier of financial risk measurement, contributing to a deeper, more nuanced understanding of the framework of market tail risk and the shadows that rare disasters cast upon it.

On the basis of the foundational insights provided by the RIX, subsequent research has attempted to decode its complexities and use its predictive power across various market scenarios. The seminal work of Du and Kapadia (2012) established a critical baseline, arguing the RIX as a key indicator for assessing the likelihood and impact of market crises. This initial investigation into the tail risks underscored the urgent need for a measure that could capture the extreme market volatility beyond the scope of conventional indices. Following this pioneering study, further studies have delved into the empirical applications and theoretical extensions of the RIX, each contributing unique perspectives on its utility and significance. For instance, Gao, Gao, and Song (2018) constructed the RIX via out-of-the-money (OTM) put options on different economic sector indices and documented its covariation with higher hedge fund returns. They found that hedge fund managers skilled in leveraging the RIX achieve superior future fund performance while being less susceptible to crisis risk. Similarly, the concept of global ex ante tail risk concerns ($GRIX$) was developed by Gao, Lu, and Song (2019) to analyze the variations in cross-sectional returns across global asset categories, thereby extending the pricing effect of the RIX on a global scale. Additionally, Liu, Chan, and Faff (2022) estimated the firm-level RIX, the firm-level jump-implied variance contribution index ($JIVX$), which effectively forecasted cross-sectional stock returns surrounding earnings announcements. These studies have demonstrated the robustness of the RIX in predicting market returns, particularly its ability to signal forthcoming downturns, as well as its adaptability as an indicator for navigating the complexities of financial markets due to its feasibility in various market conditions. Recognizing the significant empirical utility of the RIX, one recent study by Albert, Herold, and Muck (2023) introduces an advanced technique involving the risk-neutral return distribution (RND) to refine the calculation of the RIX.

Although previous studies have significantly enhanced the comprehension of the RIX, especially in its application to empirical market analysis, an essential gap persists in the academic research surrounding this measure. Most of the existing literature has focused on the empirical utility of the RIX, often at the expense of an in-depth theoretical exploration. This empirical emphasis, though valuable, has inadvertently led to a less thorough understanding of the fundamental mechanisms of the RIX. For example, none of them have displayed the time series or term structures of the RIX. Consequently, academics and practitioners are left with a somewhat superficial grasp of the RIX, aware of its importance yet they are still far from a comprehensive understanding of its core principles. Furthermore, the predominance of empirical analysis in existing research has limited the objective to correlations among observations, rather than developing a deeper understanding of the causal relationships between the RIX and other risk-neutral volatility and skewness indicators. The literature, thus far, has provided limited insight into how the RIX, as a measure, responds to and interacts with the dynamics of market tail risks. This gap is particularly noticeable in the analysis of market reactions to rare disaster risks. Although the existing literature recognizes the significance of the RIX, it rarely delves into the mathematical details that clarify its connection with higher-order risks. Such an exploration is crucial, as it would reflect the capacity of the RIX to indicate and encompass the broader spectrum of market uncertainties inherent in higher-order moments.

The need for a refined analytical framework is evident, one that surpasses empirical observations to interpret the theoretical conceptions of the RIX. This approach would not only enhance our conceptual understanding of the RIX but also enrich our comprehension of its comparative effectiveness in indicating and predicting market crashes. It is within this gap that this study positions itself, aiming to bridge the divide between empirical utility and theoretical depth, thereby offering a holistic view of the RIX and make several pivotal contributions to the field of financial risk management and market dynamics analysis.

First, we introduce an enhanced definition of the RIX. This could not only clarify the theoretical underpinnings of the RIX but also highlight its precision as an indicator of market tail risks. Compared to the original definition in Du and Kapadia (2012), our modified definition is more streamlined when utilized alongside the model-free approach. Second, our study develops an exact model of the RIX within the Gram-Charlier density framework, and draws comparisons to risks from the higher-order moments. By outlining the mathematical structure of the RIX, we explain its inherent relationship with higher-order moments, especially the risk-neutral third moment of log-returns (TM) and the risk-neutral third central moment of log-returns (TCM), providing a clear, quantitative understanding of its interaction with market dynamics. Third, by employing the time series and term structure analyses across different forward-looking horizons (30-day, 60-day, and 90-day periods), we demonstrate the temporal sensitivity of the RIX. This aspect of our study underscores the efficiency of the RIX as an indicator of the left tail risks and how the predictive power of the RIX evolves over time, offering valuable insights into its efficacy in anticipating market downside shifts across various time frames. Finally, we address the practical implications of our findings for investors, risk managers, and policymakers. By providing a more detailed perspective of the capabilities of the RIX in indicating higher-order risks, our study empowers market participants with enhanced tools for risk assessment and strategic decision-making in the face of extreme uncertainty. In sum, our research bridges the theoretical and empirical realms. We not only fulfill the existing gaps in the literature but also pave the way for future inquiries into the sophisticated dynamics of market risks and measures designed to apprehend them.

The remainder of this study is organized as follows. In Section 2, we discuss the theoretical frameworks. Then, in Section 3 we display our data and the methodology employed in this study. We present the estimation results in Section 4. Finally, we conclude this paper in Section 5. The appendices give the details of the derivations.

2 Theoretical Framework

In this section, we first introduce an enhanced definition of the RIX developed in this study, and clearly illustrate its differences from previous literature. We also state the computation of the TM, and show its relationship with the RIX. In addition, we demonstrate the model-free measures of the RIX and TM, and the exact model if the underlying follows a process based on the Gram-Charlier density. Then, following Gao, Gao, and Song (2018), and Gao, Lu, and Song (2019), we primarily concentrate on the derivation of the extreme downside risk, referred to as the lower half range of the RIX and is denoted as RIX^{-}.

2.1 Enhanced Definition of the RIX

Du and Kapadia (2012) first forwarded the construction of tail risk index as the differential impact of discontinuities on two measures of stock return variability: the variance of the log-return measured in Bakshi, Kapadia, and Madan (2003) (BKM, henceforth) and the VIX. Du and Kapadia (2012) argue that the former measures the square of summed log-returns, while the latter relates to the sum of squared log-returns (the integrated variance). However, the VIX would be biased in measuring the quadratic variation when there are extreme movements in the stock price leading to discontinuities (Carr and Wu, 2009). In contrast, the BKM variance measure can avoid the discrete sum approximation and accurately capture higher-order impact of jumps, i.e., the tail risk. Therefore, the tail risk can be clearly presented by the difference between the two measures.

This study aims to clearly clarify the reasons why the RIX can serve as an indicator of tail risks. On the basis of the Taylor series,[1] higher-order risks can be written in the following form

$$6\left(\frac{S_T}{F_t^T}-1-\ln\frac{S_T}{F_t^T}-\frac{1}{2}\ln^2\frac{S_T}{F_t^T}\right)=\ln^3\frac{S_T}{F_t^T}+O\left(\ln^4\frac{S_T}{F_t^T}\right), \tag{1}$$

where F_t^T is the forward price, T is the maturity, and t is the spot time. Although the risks beyond the fourth order are negligible and can be disregarded, it is evident that the left side of the equation effectively encompasses higher-order risks demonstrated on the right side. Hence, the definition of RIX can be developed as the risk-neutral expectation of the left terms.

Definition 1. *The definition of the rare disaster concern index, the RIX, at time t is*

$$RIX_t \equiv 6E_t^{\mathbb{Q}}\left(\frac{S_T}{F_t^T}-1-\ln\frac{S_T}{F_t^T}-\frac{1}{2}\ln^2\frac{S_T}{F_t^T}\right). \tag{2}$$

Remark 1.1. Du and Kapadia (2012) employed $JTIX$ to refer to the jump and tail index. Specifically, Du and Kapadia (2012) denoted $JTIX$ at time t as

$$JTIX_t = \mathbb{V} - \mathbb{IV} \tag{3}$$

where $\mathbb{V}$ is the BKM_2 (volatility payoff contract), and $\mathbb{IV}$ is the VIX^2. However, Du and Kapadia (2012) used the stock price S_t to compute the log-return. Consequently, there are several terms related to the risk-free rate in the calculation of the $\mathbb{IV}$, leading to a less succint expression

$$e^{-r\tau}\mathbb{IV} = \frac{2}{\tau}\left[\int_0^{S_t}\frac{1}{K^2}P_t\left(K\right)\,dK+\int_{S_t}^{\infty}\frac{1}{K^2}C_t\left(K\right)\,dK - e^{-r\tau}\left(e^{r\tau}-1-r\tau\right)\right] \tag{4}$$

[1] We start by focusing on capturing higher-order risks, which can be easily obtained via Taylor series as follows

$$\begin{aligned} e^x &= 1+x+\frac{1}{2!}x^2+\frac{1}{3!}x^3+\frac{1}{4!}x^4+\cdots \\ &= 1+x+\frac{1}{2!}x^2+\frac{1}{3!}x^3+O\left(x^4\right). \end{aligned}$$

After rearranging and substituting with the log-return with respect to the forward price, Equation (1) can be obtained.

where τ is the time to maturity $(T-t)$, K is the strike price, and $C_t(K)$ and $P_t(K)$ are the prices of OTM European call and put options at time t, respectively.

Remark 1.2. Gao, Gao, and Song (2018) is the first to use the RIX to refer to this tail risk indicator.[2] They also considered the downside versions of both $\mathbb{IV}$ and $\mathbb{V}$, which means that only OTM put options that protect investors against negative price jumps are used

$$RIX_t \equiv \mathbb{V}^- - \mathbb{IV}^- = \frac{2e^{r\tau}}{\tau}\int_0^{S_t} \frac{\ln \frac{S_t}{K}}{K^2} P_t\left(K\right) dK. \tag{5}$$

However, the RIX of Gao, Gao, and Song (2018), as well as the definition of the $GRIX$ in Gao, Lu, and Song (2019) suffer the same issue as Du and Kapadia (2012) due to the use of S_t to compute $\mathbb{IV}$.

Remark 1.3. Although we use the name of "rare disaster concern index", we opt for the forward price, F_t^T, to calculate the log-return instead of S_t. This approach allows us to set the risk-neutral expectation of the first two terms, $\dfrac{S_T}{F_t^T} - 1$, as 0. Consequently, RIX can be characterized as the difference between the risk-neutral expectations of $-\ln \dfrac{S_T}{F_t^T}$ and $-\dfrac{1}{2}\ln^2 \dfrac{S_T}{F_t^T}$, which correspond to $\mathbb{IV}$ and $\mathbb{V}$, respectively. Moreover, after applying the forward price, the annualized integrated variance can be written as

$$e^{-r\tau}\mathbb{IV} = \frac{2}{\tau}\left[\int_0^{F_t^T} \frac{1}{K^2} P_t\left(K\right) dK + \int_{F_t^T}^{\infty} \frac{1}{K^2} C_t\left(K\right) dK\right]. \tag{6}$$

Compared to Equation (4), Equation (6) is more concise as it excludes terms related to the interest rate.

Remark 1.4. There is a constant 6 in front of the entire expression, which is resulted from the coefficient of the cubic term in Taylor series, $\dfrac{1}{3!}$. Considering the negligibility of risks beyond the third-order moment, the TM can be regarded as an approximation of

[2] Although originally constructed by Du and Kapadia (2012), the study remains a working paper. Hence, we adopt the RIX notation as established by Gao, Gao, and Song (2018), which has been published in the Review of Financial Studies.

the RIX as follows

$$TM_t \equiv E_t^{\mathbb{Q}} \left(\ln^3 \frac{S_T}{F_t^T} \right) \approx RIX_t. \tag{7}$$

Then, we investigate the relationship between the RIX and TM. It is obvious that our definition of the RIX, subtracting $\mathbb{V}$ from $\mathbb{IV}$, is opposite to the previous studies (e.g., Du and Kapadia, 2012; Gao, Gao, and Song, 2018; Gao, Lu, and Song, 2019). This departure results from the observation that the option market exhibits negative skewness, suggesting that risks associated with the tail end should similarly be negative.

2.2 Model-Free Measure of the RIX

According to Carr and Madan (2001) and BKM, any twice-differentiable payoff function with bounded expectation can be spanned by a continuum of OTM European options, bonds, and shares. For payoff function $H(x) \in \mathscr{C}^2$ and some constant x_0, the decomposed payoff function is given by

$$\begin{aligned} H(x) = H(x_0) + H_x(x_0)(x - x_0) &+ \int_0^{x_0} H_{xx}(K)\, P_T(K)\, dK \\ &+ \int_{x_0}^{\infty} H_{xx}(K)\, C_T(K)\, dK \end{aligned} \tag{8}$$

where $C_T(K)$ and $P_T(K)$ are the prices of OTM European call and put options at maturity. Therefore, the model-free measure of the RIX can be simply obtained by using Equation (8) on Equation (2), which is the static replication of the RIX. Similarly, the model-free measure of the TM is applying Equation (8) to Equation (7).

Proposition 1. *The model-free measure of the RIX at time t is*

$$RIX_t = e^{r\tau} \left[\int_0^{F_t^T} \frac{6}{K^2} \ln \frac{K}{F_t^T} P_t(K)\, dK + \int_{F_t^T}^{\infty} \frac{6}{K^2} \ln \frac{K}{F_t^T} C_t(K)\, dK \right]. \tag{9}$$

The model-free measure of the TM at time t is

$$TM_t = e^{r\tau} \left[\int_0^{F_t^T} \left(\frac{6}{K^2} \ln \frac{K}{F_t^T} - \frac{3}{K^2} \ln^2 \frac{K}{F_t^T} \right) P_t(K)\, dK + \int_{F_t^T}^{\infty} \left(\frac{6}{K^2} \ln \frac{K}{F_t^T} - \frac{3}{K^2} \ln^2 \frac{K}{F_t^T} \right) C_t(K)\, dK \right]. \tag{10}$$

The derivations are shown in Appendix A.

Remark 1.1. To make the equations more concise, $Q_t(K)$ is designated to represent all OTM European options at time t. Then, Equation (9) and Equation (10) can be simplified to the following forms

$$RIX_t = e^{r\tau} \int_0^\infty \frac{6}{K^2} \ln \frac{K}{F_t^T} Q_t(K)\, dK,$$
$$TM_t = e^{r\tau} \int_0^\infty \left(\frac{6}{K^2} \ln \frac{K}{F_t^T} - \frac{3}{K^2} \ln^2 \frac{K}{F_t^T} \right) Q_t(K)\, dK.$$

Remark 1.2. The values of the two model-free measures are slightly different. After taking the risk-neutral expectation, we can obtain the difference, which represents the risks associated with higher-order moments beyond the third.[3]

2.3 The RIX under the Gram-Charlier Density

Due to the ease of expressing skewness and kurtosis under the Gram-Charlier density, we intend to use this special density function to further investigate the RIX. According to Zhang and Xiang (2008), and Aschakulporn and Zhang (2022a), the stock price, S_T, can be modeled by

$$S_T = F_t^T e^{\left(-\frac{1}{2}\sigma^2 + \mu_c\right)\tau + \sigma\sqrt{\tau} y} \tag{11}$$

where σ, μ_c, and y is the standard deviation, convexity adjustment term, and a random variable, respectively. Using the Gram-Charlier density, if y has probability density

$$f(y) = n(y) - \frac{\lambda_1}{3!} \frac{d^3 n(y)}{dy^3} + \frac{\lambda_2}{4!} \frac{d^4 n(y)}{dy^4} \tag{12}$$

where $n(y) = \frac{1}{\sqrt{2\pi}} e^{-\frac{y^2}{2}}$, then y will have a mean of zero, variance of one, skewness equal to λ_1, and an excess kurtosis of λ_2. The forward price, F_t^T, is related to the current stock price, S_t, by $F_t^T = S_t e^{(r-q)\tau}$, where r is the risk-free rate, and q is the dividend yield. The convexity adjustment term is required to keep this model arbitrage-free by ensuring that

[3] Risks from the fourth or higher-order moments are worthy of exploration. However, our main concern is the conception of the RIX.

the stock price satisfies the martingale condition, $F_t^T = E_t^{\mathbb{Q}}(S_T)$, in the risk-nuetral world and was be found to be

$$\mu_c = -\frac{1}{\tau}\ln\left[1 + \frac{\lambda_1}{3!}\left(\sigma\sqrt{\tau}\right)^3 + \frac{\lambda_2}{4!}\left(\sigma\sqrt{\tau}\right)^4\right]. \tag{13}$$

Then, it is easy to prove that the third central moment of the log-return under the Gram-Charlier density, TCM, is $(\sigma\sqrt{\tau})^3\lambda_1$. After combining with Equation (2), Proposition 2, the exact model of the RIX under the Gram-Charlier density can be obtained.

Proposition 2. *The exact model of the RIX under the Gram-Charlier density at time t is*

$$RIX_t = -3\left(-\frac{1}{2}\sigma^2 + \mu_c\right)^2 \tau^2 - 6\mu_c\tau. \tag{14}$$

The derivation is shown in Appendix B.

Remark 2.1. Aschakulporn and Zhang (2022a) stated the annualized RIX under the Gram-Charlier density in their Appendix C as

$$RIX_t = \left(r - q - \frac{1}{2}\sigma^2 + \mu_c\right)^2 \tau + 2\mu_c. \tag{15}$$

Since Aschakulporn and Zhang (2022a) employed S_t rather than the forward price F_t^T to compute the log-return, the model includes two additional terms, r and q, which are related to S_t. The RIX developed by us is opposite to previous studies and is three times larger, which are explained in Definition 1. Also, by using F_t^T, we keep the derivations in this study consistant.

Remark 2.2. The TM at time t can also be derived by combining the Gram-Charlier density with Equation (7)

$$TM_t = \left(-\frac{1}{2}\sigma^2 + \mu_c\right)^3 \tau^3 + 3\left(-\frac{1}{2}\sigma^2 + \mu_c\right)(\sigma\tau)^2 + \left(\sigma\sqrt{\tau}\right)^3 \lambda_1. \tag{16}$$

The derivation is shown in Appendix C.

Remark 2.3. To show the differences between the RIX and TM more clearly, we perform a Taylor expansion on Equations (14) and (16) and get the following results

$$
\begin{aligned}
RIX_t =& \lambda_1 \left(\sigma\sqrt{\tau}\right)^3 + \frac{1}{4}\left(\lambda_2 - 3\right)\left(\sigma\sqrt{\tau}\right)^4 + O\left(\sigma\sqrt{\tau}\right)^5, \\
TM_t =& \lambda_1 \left(\sigma\sqrt{\tau}\right)^3 - \frac{3}{2}\left(\sigma\sqrt{\tau}\right)^4 + O\left(\sigma\sqrt{\tau}\right)^5.
\end{aligned}
$$

Although the first term of the expanded RIX and TM are the same, giving the TCM, the crucial distinction lies in the inclusion of terms beyond the third-order, which is included in the RIX.

Remark 2.4. It can be inferred that the RIX is a function of the skewness and kurtosis referring to Equations (13), (14), and (16). After accounting for the Gram-Charlier positive-definite boundary argued in Aschakulporn and Zhang (2022), Figure 1 displays the relationships among the RIX, TM, and TCM, with the setting of $\sigma = 0.2$, $\tau = 1/12$, and $\lambda_2 = 2, 2.5, 3$, and 3.5, based on Equations (14) and (16), respectively. The negligible divergences observed among the RIX, TM, and TCM signify their similarity in capturing the third moment risks. Additionally, the RIX also accounts for risks from higher moments, reflecting its robustness as an indicator of the tail risks.

[Insert Figure 1 about here.]

2.4 Downside Risk of the RIX^-

According to existing literature, market crashes draw more attention from investors compared to a bull market. Since tail risk concerns with the extreme downside jumps can be computed by OTM puts, the RIX^-, which refers to the lower half range of the RIX, is easily obtained through the model-free measure. The formula of the RIX^- under the Gram-Charlier density can also be derived through the risk-neutral expectation of OTM puts, then, the parameters can be estimated. Moreover, the relationship between the RIX^- and TM^- is also of interest for us to explore.

On the basis of Equation (9), the model-free measure of the RIX^- at time t can be inferred to be the second term related to the OTM put options

$$RIX_t^- = e^{r\tau} \int_0^{F_t^T} \frac{6}{K^2} \ln \frac{K}{F_t^T} P_t(K)\, dK, \tag{17}$$

which is also applicable to the TM^-

$$TM_t^- = e^{r\tau} \int_0^{F_t^T} \left(\frac{6}{K^2} \ln \frac{K}{F_t^T} - \frac{3}{K^2} \ln^2 \frac{K}{F_t^T} \right) P_t(K)\, dK. \tag{18}$$

Moreover, the probability of downside risk occurring will be the probability that the stock price is lower than the forward price, $P(S_T < F_t^T) = E\left(\mathbb{1}_{S_T < F_t^T}\right)$. Consequently, the RIX^- is the combination of the indicator function and Equation (2), and is composed of three components. The three components are the current value of a European put option, semi-expectation of the log-return, and semi-second moment of the log-return as follows

$$RIX_t^- = -\frac{6}{F_t^T} E_t^{\mathbb{Q}} \left[\max\left(F_t^T - S_T, 0\right) \right] - 6E_t^{\mathbb{Q}} \left(\ln \frac{S_T}{F_t^T} \times \mathbb{1}_{S_T < F_t^T} \right) - 3E_t^{\mathbb{Q}} \left(\ln^2 \frac{S_T}{F_t^T} \times \mathbb{1}_{S_T < F_t^T} \right). \tag{19}$$

Based on Equation (11), it must satisfy $y < -\frac{\left(-\frac{1}{2}\sigma^2 + \mu_c\right)\sqrt{\tau}}{\sigma}$ under the Gram-Charlier density to guarantee that $S_T < F_t^T$. We set $d_2 = \frac{\left(-\frac{1}{2}\sigma^2 + \mu_c\right)\sqrt{\tau}}{\sigma}$, so the RIX^- is an indicator of potential market crashes only when $y < -d_2$. Then, the exact model of the RIX^- can be obtained by rewriting Equation (19) under the Gram-Charlier density.

Proposition 3. *RIX^- under the Gram-Charlier density at time t is*

$$RIX_t^- = A + B\beta_0 + C\beta_1 + D\beta_2 \tag{20}$$

where

$$
\begin{aligned}
A &= -6\left[N(d_1) - N(d_2) + n(d_2)\left(\frac{\lambda_1}{3!}E + \frac{\lambda_2}{4!}F\right)\sigma\sqrt{\tau}\right],\\
B &= -6\left(-\frac{1}{2}\sigma^2 + \mu_c\right)\tau - 3\left(-\frac{1}{2}\sigma^2 + \mu_c\right)^2\tau^2,\\
C &= -6\sigma\sqrt{\tau} - 6\left(-\frac{1}{2}\sigma^2 + \mu_c\right)\sigma\left(\sqrt{\tau}\right)^3, \qquad D = -3\sigma^2\tau,\\
E &= -\left(d_2 - \sigma\sqrt{\tau}\right), \qquad F = -\left(1 - d_2^2 + \sigma\sqrt{\tau}d_2 - \sigma^2\tau\right),\\
d_2 &= \frac{\left(-\frac{1}{2}\sigma^2 + \mu_c\right)\tau}{\sigma\sqrt{\tau}}, \qquad d_1 = d_2 + \sigma\sqrt{\tau},\\
\beta_0 &= N(-d_2) + \frac{\lambda_1}{3!}(-d_2^2 + 1)n(-d_2) + \frac{\lambda_2}{4!}(d_2^3 - 3d_2)n(-d_2),\\
\beta_1 &= -n(-d_2) + \frac{\lambda_1}{3!}d_2^3 n(-d_2) + \frac{\lambda_2}{4!}(-d_2^4 + 2d_2^2 + 1)n(-d_2),\\
\beta_2 &= d_2 n(-d_2) + N(-d_2) + \frac{\lambda_1}{3!}(-d_2^4 - d_2^2 - 2)n(-d_2) + \frac{\lambda_2}{4!}(d_2^5 - d_2^3)n(-d_2).
\end{aligned}
$$

The derivation is shown in Appendix D.

Remark 3.1. The pricing formula of a European call option with skewness and kurtosis has been proposed by Aschakulporn and Zhang (2022a) as

$$
c_t = F_t^T e^{-r\tau}N(d_3) - Ke^{-r\tau}N(d_4) + Ke^{-r\tau}n(d_4)\left(\frac{\lambda_1}{3!}E + \frac{\lambda_2}{4!}F\right)\sigma\sqrt{\tau} \tag{21}
$$

where

$$
\begin{aligned}
E &= -\left(d_4 - \sigma\sqrt{\tau}\right), \qquad F = -\left(1 - d_4^2 + \sigma\sqrt{\tau}d_4 - \sigma^2\tau\right),\\
d_4 &= \frac{\ln\left(F_t^T/K\right) + \left(-\frac{1}{2}\sigma^2 + \mu_c\right)\tau}{\sigma\sqrt{\tau}}, \qquad d_3 = d_4 + \sigma\sqrt{\tau}.
\end{aligned}
$$

As for the value of a European put option, it can be easily computed by using the put-call parity, $c_t(K) - p_t(K) = F_t^T e^{-r\tau} - Ke^{-r\tau}$. Once the forward price is equal to the strike price, we get $c_t(F_t^T) = p_t(F_t^T) = e^{-r\tau}E_t^{\mathbb{Q}}\left[p_T\left(F_t^T\right)\right]$. Additionally, d_4 is exactly the same as d_2 when F_t^T is equal to K. Therefore, the first term of Equation (19) can be determined to be

$$
-\frac{6}{F_t^T}E_t^{\mathbb{Q}}\left[\max\left(F_t^T - S_T, 0\right)\right] = -\frac{6}{F_t^T}e^{r\tau}p_t(F_t^T) = -\frac{6}{F_t^T}e^{r\tau}c_t(F_t^T)
$$

where F_t^T is equal to K.

Remark 3.2. According to Equation (11), the log-return under the Gram-Charlier density is

$$\ln \frac{S_T}{F_t^T} = \left(-\frac{1}{2}\sigma^2 + \mu_c\right)\tau + \sigma\sqrt{\tau}y.$$

Therefore, the last two terms of Equation (19) are associated with the risk-neutral expectation of y and the indicator function. To enhance conciseness of formula, we employ β_n to refer to $E_t^{\mathbb{Q}}\left(y^n \times \mathbb{1}_{S_T<F_t^T}\right)$, respectively. More specifically, we denote β_0, β_1, and β_2 as semi-probability, semi-expectation of y, and semi-second moment of y.

Remark 3.3. The TM^- under the Gram-Charlier density can be easily obtained. The only difference compared to the RIX^- is the semi-expectation of y^3, $E_t^{\mathbb{Q}}\left(y^3 \times \mathbb{1}_{S_T<F_t^T}\right)$, which is denoted as β_3. Consequently, β_3 can be regarded as the semi-third moment of y, and the exact model of the TM^- at time t is as follows

$$TM_t^- = G\beta_0 + H\beta_1 + I\beta_2 + J\beta_3 \tag{22}$$

where

$$\begin{aligned}
&G = \left(-\frac{1}{2}\sigma^2 + \mu_c\right)^3 \tau^3, \qquad H = 3\left(-\frac{1}{2}\sigma^2 + \mu_c\right)^2 \sigma\left(\sqrt{\tau}\right)^5,\\
&I = 3\left(-\frac{1}{2}\sigma^2 + \mu_c\right)\sigma^2\tau^2, \qquad J = \sigma^3\left(\sqrt{\tau}\right)^3,\\
&\beta_3 = (-d_2^2 - 2)n(-d_2) + \frac{\lambda_1}{3!}[(d_2^5 + 2d_2^3 + 6d_2)n(-d_2) + 6N(-d_2)] + \frac{\lambda_2}{4!}(-d_2^6 - 3d_2^2 - 6)n(-d_2).
\end{aligned}$$

The derivation is shown in Appendix E.

Remark 3.4. Similarly, after accounting for the Gram-Charlier positive-definite boundary argued in Aschakulporn and Zhang (2022), Figure 2 displays the relationship between the RIX^- and TM^-, with the setting of $\sigma = 0.2$, $\tau = 1/12$, and $\lambda_2 = 2, 2.5, 3$, and 3.5, based on Equations (20) and (22), respectively. Compared with Figure 1, Figure 2 reveals that the RIX^- and TM^- are significantly closer, indicating that the third moment risks contribute more substantially during periods of adverse market movements compared to the other higher-order risks. The results also show the superior performance of the RIX^- particularly as an indicator of the left tail risks.

[Insert Figure 2 about here.]

3 Data and Methodology

Our aim is to enhance the comprehension of the RIX, which has been used as a proxy for tail risks in several studies (e.g., Gao, Gao, and Song, 2018; Gao, Lu, and Song, 2019; Liu, Chan, and Faff, 2022). However, none of these articles present the time series of the RIX, instead directly employing it in empirical research, leading to an incomplete perception of the RIX. This study has numerically revealed the essence of the RIX along with its relationships with the TM and TCM. To present the RIX clearly, we will construct the time series and term structure based on the market data in this section.

3.1 Data

We opt for SPX options, traded on the CBOE, as the primary sample to generate the time series of the RIX. This selection enables us to directly compare the RIX with the VIX and $SKEW$ listed on the CBOE since the underlying of these indices is the same. Daily transaction data for SPX options are provided by OptionMetrics, and the values of the VIX and $SKEW$ are collected from the CBOE. For our analysis, we exclusively retain monthly trading options, while weekly trading options are omitted. The dataset encompasses the entirety of the COVID-19 pandemic, ranging from 1 January, 2020 to 28 February, 2023, a period marked by significant economic downturns. Daily interest rates are derived via linearly interpolation and extrapolation of the US Treasury yield rates, as sourced from the U.S. Department of the Treasury website. The data are screened following the filters outlined in the CBOE VIX White Paper,[4] ensuring consistancy with the VIX and $SKEW$. The forward price, F_t^T, is also computed following the CBOE VIX White Paper.

[4] The CBOE VIX White Paper is `https://cdn.cboe.com/api/global/us_indices/governance/Volatility_Index_Methodology_Cboe_Volatility_Index.pdf`.

3.2 Methodology

After filtering based on the CBOE VIX White Paper, the screened data is used to calculate the time series and term structure of the RIX based on the model-free measures as detailed in Equation (9). However, direct integration is not possible due to the inherent constraints of limited trading option strike prices. The trapezium rule (viz. trapezoidal integration) is widely employed to counter this issue by approximating the definite integral within the confines market data (Dennis and Mayhew, 2002; Jiang and Tian, 2005; Conrad, Dittmar, and Ghysels, 2013; Neumann and Skiadopoulos, 2013; Chang, Christoffersen, and Jacobs, 2013; Chatrath et al., 2016; Stilger, Kostakis, and Poon, 2017; Ruan and Zhang, 2018; Liu, Chan, and Faff, 2022). Consequently, applying the trapezium rule to Equation (9), the integral can be discretized to

$$RIX_t = 6e^{r\tau} \sum_{i=1}^{\infty} \frac{\Delta K_i}{K_i^2} \ln \frac{K_i}{F_t^T} Q(K_i) \tag{23}$$

where

$$\Delta K_i = \begin{cases} K_2 - K_1, & i = 1 \\ \frac{1}{2}\left(K_{i+1} - K_{i-1}\right), & 1 < i < n \\ K_n - K_{n-1}, & i = n \end{cases} \tag{24}$$

and n is the number of strikes. Equation 24 is defined in the CBOE VIX White Paper. Similarly, the same procedure can also be applied to Equation (10) and we have

$$TM_t = 3e^{r\tau} \sum_{i=1}^{\infty} \frac{\Delta K_i}{K_i^2} \left(2\ln \frac{K_i}{F_t^T} - \ln^2 \frac{K_i}{F_t^T}\right) Q(K_i). \tag{25}$$

Moreover, we also replicate the time series of the TCM, $JTIX$, VIX, $SKEW$, and different payoff contracts stated in BKM. Specifically, the BKM_n corresponds to the values of $E_t^{\mathbb{Q}}\left(R_\tau^n\right)$, where R_τ is the log-returns $\ln \frac{S_T}{F_t^T}$.[5] The computations of these indices

[5] The mean is approximated in BKM by setting the dividend yield, q, to zero:

$$E_t^{\mathbb{Q}}\left(R_\tau\right) = \mu_\tau = e^{r\tau} - 1 - \frac{1}{2!}E_t^{\mathbb{Q}}\left(R_\tau^2\right) - \frac{1}{3!}E_t^{\mathbb{Q}}\left(R_\tau^3\right) - \frac{1}{4!}E_t^{\mathbb{Q}}\left(R_\tau^4\right).$$

using trapezium rule are[6]

$$BKM_{2_t} = E_t^{\mathbb{Q}}\left(R_\tau^2\right) = 2e^{r\tau}\sum_{i=1}^{\infty}\frac{\Delta K_i}{K_i^2}\left(1 - \ln\frac{K_i}{F_t^T}\right)Q(K_i), \tag{26}$$

$$BKM_{3_t} = E_t^{\mathbb{Q}}\left(R_\tau^3\right) = 3e^{r\tau}\sum_{i=1}^{\infty}\frac{\Delta K_i}{K_i^2}\left(2\ln\frac{K_i}{F_t^T} - \ln^2\frac{K_i}{F_t^T}\right)Q(K_i),^{7} \tag{27}$$

$$BKM_{4_t} = E_t^{\mathbb{Q}}\left(R_\tau^4\right) = 4e^{r\tau}\sum_{i=1}^{\infty}\frac{\Delta K_i}{K_i^2}\left(3\ln^2\frac{K_i}{F_t^T} - \ln^3\frac{K_i}{F_t^T}\right)Q(K_i), \tag{28}$$

$$BKM_{1_t} = E_t^{\mathbb{Q}}\left(R_\tau\right) = e^{r\tau} - 1 - \frac{BKM_{2_t}}{2} - \frac{BKM_{3_t}}{6} - \frac{BKM_{4_t}}{24}, \tag{29}$$

$$VIX_t^2 = 2e^{r\tau}\sum_{i=1}^{\infty}\frac{\Delta K_i}{K_i^2}Q(K_i), \tag{30}$$

$$JTIX_t = BKM_{2_t} - VIX_t^2, \tag{31}$$

$$TCM_t = BKM_{3_t} - 3BKM_{1_t} \times BKM_{2_t} + 2BKM_{1_t}^3, \tag{32}$$

$$Var_t = BKM_{2_t} - BKM_{1_t}^2, \tag{33}$$

$$skewness_t = \frac{TCM_t}{Var_t^{\frac{3}{2}}}, \tag{34}$$

$$VIX_t = 100\sqrt{\frac{VIX_t^2}{\tau}}, \tag{35}$$

$$SKEW_t = 100 - 10 \times skewness_t. \tag{36}$$

The errors of estimators have been researched in several studies (Jiang and Tian, 2005; Jiang and Tian, 2007; Aschakulporn and Zhang, 2022b). Two primary sources of errors have been identified: truncation and discretization errors. The truncation errors arise from the finite range of strike prices available in the option market. Therefore, the bounds of integration would change from $K \in (0, \infty)$ to $K \in [K_{min}, K_{max}]$. According to Aschakulporn and Zhang (2022), a boudary controlling factor, a, is introduced as

$$[K_{min}, K_{max}] := [F_t^T \times a, F_t^T / a] \tag{37}$$

[6] We also calculate the time series for indices focusing solely on the downside risk with OTM options, designated as RIX^-, TM^-, TCM^-, BKM_2^-, BKM_3^-, BKM_4^-, BKM_1^-, VIX^{2^-}, and $JTIX^-$.

[7] BKM_3 is the same as TM since they are both the risk-neutral expectation of the cube of the log-return.

where $a \in (0, 1)$. Thus, as a approaches 0, K_{min} and K_{max} would approach 0 and ∞, respectively, fulfilling the integral bounds. Conversely, as a approaches 1, the strike prices would align with the at-the-money (ATM) condition. As for the discretization errors, they come from the application of the trapezium rule, which is required as the market strikes are discrete and the difference is ΔK.

These errors can be mitigated through interpolation and extrapolation techniques. Aschakulporn and Zhang (2022) estimate the BKM skewness using a variety of interpolation and extrapolation methods, including constant, linear, cubic spline, and Gaussian kernel approaches, and compare these estimators with the true model based value computed via stochastic volatility and contemporaneous jumps (SVCJ) model developed by Duffie, Pan, and Singleton (2000). Subsequently, they discover that linear interpolation of the implied volatility curve, coupled with constant extrapolation using $\Delta K = 0.05\% \times F_t^T$ and $a = 0.25$, yields the most reliable skewness estimation within 10^{-3} of the true value. Consequently, we adopt this configuration for the construction of our indices. Figures 3 and 4 compare the CBOE VIX and $SKEW$ to the VIX and $SKEW$ estimated using the aforementioned approaches. Despite the replication not being identical, the estimations closely approximate the CBOE indices, as shown by the correlations of 0.99 and 0.97 for the VIX and $SKEW$, respectively. This signifies that the deviations are insignificant, supporting the feasibility of the method. Therefore, we use the estimated values as benchmarks to proceed with our investigation.

[Insert Figure 3 about here.]

[Insert Figure 4 about here.]

4 Results

In this section, we present the time series and term structures of the indices we constructed and analyze their relationships with the RIX.

4.1 The RIX with the CBOE VIX and $SKEW$

First, we compare the CBOE VIX and $SKEW$ following the CBOE SKEW White Paper.[8] The CBOE argues that the anticipation of market participants concerning a catastrophic market drop, often referred to as a "black swan" event, significantly influences perceived tail risk. Figure 5 shows that during the COVID-19 pandemic, the VIX reached its peak of 82.69% on 16 March, 2020 within the sample period in a contemporaneous setting where the $SKEW$ was relatively low at 114.66.

[Insert Figure 5 about here.]

Figure 6 illustrates that the VIX, before reaching extreme values over 40, is associated with both low and high levels of the $SKEW$. This observation suggests that there is variability in market perceptions and reactions to risk before the VIX indicator signals a state of extreme market volatility. However, as the VIX increases beyond 40, indicating extreme market turbulence, the range of the $SKEW$ values tends to narrow. The CBOE's explanation suggests that after a significant market downturn, the market's expectation for another immediate drop diminishes. This could be due to the initial market shock adjusting investors' expectations and risk assessments, leading to a recalibration of perceived future tail risks. Essentially, once the market has absorbed the impact of a major downturn, the anticipation of further immediate declines is reduced, as participants might view the most immediate risks as already realized.

[Insert Figure 6 about here.]

[8] The CBOE $SKEW$ White Paper is `https://cdn.cboe.com/resources/indices/documents/SKEWwhitepaperjan2011.pdf`.

Contrastingly, Figures 7 and 8 illustrate a distinctly different relationship between the VIX and RIX_{30} in comparison to the relationship observed between the CBOE VIX and $SKEW$. Serving as a proxy for tail risks, the RIX_{30} and VIX exhibit corresponding trends within the same periods, opposite to the behavior of the CBOE $SKEW$. This divergence lies in the intrinsic association between the $SKEW$ and VIX, rooted in their conceptual framework. More specifically, the $SKEW$ can be characterized as approximating an inverse square root relationship with the VIX, a functional dependency that mirrors the graphical representation observed in Figure 6. As the VIX increases, the value of the $SKEW$ would decrease, suggesting that expectations of extreme negative tail events become less pronounced as immediate market volatility rises. Therefore, instead of directly comparing the RIX with the VIX or $SKEW$, our analysis shifts to comparing the RIX against the VIX^2 and TCM.

[Insert Figure 7 about here.]

[Insert Figure 8 about here.]

4.2 The RIX with $JTIX$

As introduced by Du and Kapadia (2012), the $JITX$ is computed by Equation (31), which is the difference between the BKM_2 and VIX^2, and constitutes one third of our RIX. Subsequently, we conduct a comparative analysis among the RIX, BKM_2, and VIX^2, focusing on a 30-day term structure. Figure 9 shows that the two measures of stock return variability, the BKM_2 and VIX^2, exhibit similar patterns, with the former consistently exceeding the latter. Nevertheless, at each peak, the discrepancy between the BKM_2 and VIX^2 is significantly greater compared to their differences at lower levels, thereby highlighting an escalation in potential tail risks as represented by the $JTIX$. This phenomenon emphasizes the dynamics between market volatility and tail risk perceptions, providing a robust framework for analyzing market fluctuations and their implications on risk assessment. Moreover, the interplay between the BKM_2 and VIX^2 substantiates the contemporaneous nature of the second moment risk with higher-order risks, which is supported by Figure 10.

[Insert Figure 9 about here.]

[Insert Figure 10 about here.]

This phenomenon becomes more pronounced when attention is narrowed to the lower half range, as illustrated by Figures 11 and 12. Concentrating on the lower half range emphasizes the extremities of market behaviors, where the BKM_2 and VIX^2, and their divergence, are likely more accentuated. This focused analysis reveals the heightened sensitivity of the BKM_2 and VIX^2 to adverse market conditions, further clarifying the escalated potential for tail risks as indicated by the RIX. By focusing on this segment, the figures underscore the significant disparities between standard volatility measures and the acute stress indicators in the market's lower distribution, offering a deeper understanding of the mechanisms that drive market extremes and the inherent risks associated with them. This approach not only highlights the critical relationship between the traditional volatility and extreme adverse risk but also demonstrates how specific market conditions can amplify the perceived risk, thereby providing a clearer picture of market vulnerabilities.

[Insert Figure 11 about here.]

[Insert Figure 12 about here.]

4.3 The RIX with TM and TCM

Following the comparison of the second moment risks, we proceed to analyze the efficiency of the RIX in encompassing the third moment risks. Figure 13 displays that the RIX effectively cover the TM and TCM as evidenced by their nearly identical values, which are threefold the values of the $JTIX$. This congruence highlights the comprehensive nature of the RIX in reflecting skewness and asymmetry inherent in third moment risks. The robust alignment between the RIX and higher-order moments is further emphasized when the analysis is narrowed to focus on the downside risks with higher values, as demonstrated in Figure 14. Even in this focused view, which pays attention to the market's response to adverse conditions, the RIX^- maintains its effectiveness in mirroring the behavior of the TM and TCM. This persistence underlines the utility of the RIX as a holistic measure that effectively integrates various dimensions of market risk, offering valuable insights into the underlying dynamics of market distributions, particularly in indicating the essence of tail risks and market downturns.

[Insert Figure 13 about here.]

[Insert Figure 14 about here.]

In addition, we illustrate the differences among the RIX, TM, and TCM in Figure 15 spanning the entire range and Figure 16 for the lower half range specifically. Observations indicate that the differences between the TM and TCM are comparatively minor, even when potential tail risks increase, which is consistent with our numerical results in Section 2. Conversely, the divergences between the RIX and TM, as well as the RIX and TCM, while modest under standard market conditions, tend to widen during periods of rising risks. Intriguingly, these differences contract when the analysis is strictly limited to the lower half range, signifying that the RIX possesses a heightened proficiency in encapsulating market downside risks.

[Insert Figure 15 about here.]

[Insert Figure 16 about here.]

This phenomenon underscores the nuanced capability of the RIX as an indicator to more accurately reflect the severity and likelihood of negative market outcomes, particularly in scenarios characterized by elevated tail risks. The comparative analysis reveals that while the TM and TCM offer valuable insights into the skewness and dispersion of returns, the RIX provides a more comprehensive gauge of downside risk, indicating both the frequency and magnitude of extreme market downturns. The reduction in discrepancies specifically within the lower half range context further emphasizes the critical role of the RIX in risk management and assessment strategies, particularly for stakeholders focused on mitigating potential losses during turbulent market periods.

4.4 Term Structures of the RIX

We also present the term structures of the RIX across various durations—30-day, 60-day, and 90-day periods—to analyze how it behaves over different forward-looking horizons. As demonstrated in both Figures 17 and 18, although the RIX^- consistently exceeds the RIX in value across all observed periods, both tend to exhibit higher values as the length of the forward-looking horizon extends. This feature suggests a critical insight into the nature of the RIX as a risk measure: its sensitivity to the temporal dimension of risk assessment, since the increase in the RIX with longer horizons reflects growing uncertainty. Intuitively, the market's anticipation of future tail risk becomes more pronounced over longer durations, possibly due to the accumulation of unforeseen factors and the compounding effect of risk over time. Such observations highlight the importance of considering the time dimension in the assessment of market risks. For practitioners and researchers alike, understanding the term structure of the RIX provides valuable insights into the dynamic nature of market risk and its implications for strategic planning and risk management, as highlighted in prior studies (Gao, Gao, and Song, 2018; Gao, Lu, and Song, 2019; Liu, Chan, and Faff, 2022).

[Insert Figure 17 about here.]

[Insert Figure 18 about here.]

Additionally, we explore the variations within different ranges of the RIX utilizing a

30-day term structure, as illustrated in Figure 19. Reasonably, the RIX^+, calculated from OTM calls based on Equation (23) and representing essentially the difference between the RIX and RIX^-, is found to be positive yet significantly smaller than the absolute values of the RIX and RIX^-. This outcome suggests that the RIX^-, by capturing a broader spectrum of negative market movements, is particularly feasible for quantifying extreme downside risks. The differentiation between the RIX^+ and RIX^- underlines the nuanced dynamics of market risk, where the RIX^- serves as a more sensitive indicator of adverse market conditions. The relative smallness of the RIX^+ highlights its specific role in the risk measurement framework, potentially indicating lesser concern for extreme positive market movements compared to the pronounced focus on negative shifts.

[Insert Figure 19 about here.]

5 Conclusion

In conclusion, our study embarks on a comprehensive journey to demystify the RIX, a critical indicator in understanding and quantifying market tail risks. Through the lens of both theoretical innovation and numerical scrutiny, we have shed light on the multifaceted nature of the RIX and its integral role in capturing the nuances of extreme market volatility. By redefining the RIX and developing its exact model within the Gram-Charlier density framework, we have not only enhanced its mathematical robustness but also its interpretive clarity, offering a deeper insight into the underpinnings of market behaviors.

Our exploration also reveals the dynamic interplay between the the RIX and other indices, establishing the comparative advantage of the RIX in encapsulating market extreme uncertainties beyond conventional volatility measures. The temporal analysis across different forward-looking horizons further underscores the predictive flexibility of the RIX, affirming its significance in strategic risk management and investment decision-making.

The comparisons among the RIX and third-order risks, especially within the lower half range, highlight the exceptional capability of the RIX in signaling potential downturns and its sensitivity to the possibility of rare disasters. Such insights are invaluable for investors, risk managers, and policymakers aiming to navigate the complexities of financial markets.

Moving forward, this study lays a foundational stone for future research, encouraging a deeper examination of the RIX and its applications in diverse market conditions. The bridging of theoretical depth with empirical analysis opens new avenues for understanding the intricacies of market risk and constructs an indicator that engages both scholars and practitioners.

Disclosure Statement

The authors have declared no conflict of interest.

Data Availability Statement

Option data that support the findings of this study are available from OptionMetrics via the Wharton Research Data Services (WRDS) platform at `https://wrds-www.wharton.upenn.edu/pages/get-data/optionmetrics/` with the permission. The VIX and $SKEW$ are openly available from the CBOE website at `https://www.cboe.com/`. The US Treasury yield rate is openly available from the U.S. Department of the Treasury website at `https://home.treasury.gov/`.

References

Albert, Pascal, Michael Herold, and Matthias Muck, 2023, Estimation of rare disaster concerns from option prices—An arbitrage-free RND-based smile construction approach, *Journal of Futures Markets* 43(12), 1807–1835.

Aschakulporn, Pakorn, and Jin E. Zhang, 2022a, Bakshi, Kapadia, and Madan (2003) risk-neutral moment estimators: A Gram–Charlier density approach, *Review of Derivatives Research* 25(3), 233–281.

Aschakulporn, Pakorn, and Jin E. Zhang, 2022b, Bakshi, Kapadia, and Madan (2003) risk-neutral moment estimators: An affine jump-diffusion approach, *Journal of Futures Markets* 42(3), 365–388.

Bakshi, Gurdip, Nikunj Kapadia, and Dilip Madan, 2003, Stock return characteristics, skew laws, and the differential pricing of individual equity options, *Review of Financial Studies* 16(1), 101–143.

Carr, P., and D. Madan, 2001, Optimal positioning in derivative securities, *Quantitative Finance* 1(1), 19–37.

Carr, Peter, and Liuren Wu, 2009, Variance risk premiums, *Review of Financial Studies* 22(3), 1311–1341.

Chang, Bo Young, Peter Christoffersen, and Kris Jacobs, 2013, Market skewness risk and the cross section of stock returns, *Journal of Financial Economics* 107(1), 46–68.

Chatrath, Arjun, Hong Miao, Sanjay Ramchander, and Tianyang Wang, 2016, An examination of the flow characteristics of crude oil: Evidence from risk-neutral moments, *Energy Economics* 54, 213–223.

Conrad, Jennifer, Robert F. Dittmar, and Eric Ghysels, 2013, Ex ante skewness and expected stock returns, *Journal of Finance* 68(1), 85–124.

Dennis, Patrick, and Stewart Mayhew, 2002, Risk-neutral skewness: Evidence from stock options, *Journal of Financial and Quantitative Analysis* 37(3), 471–493.

Du, Jian, and Nikunj Kapadia, 2012, The tail in the volatility index, *U. Massachusetts, Amherst Work. Pap.*

Duffie, Darrell, Jun Pan, and Kenneth Singleton, 2000, Transform analysis and asset pricing for affine jump-diffusions, *Econometrica* 68(6), 1343–1376.

Gao, George P., Pengjie Gao, and Zhaogang Song, 2018, Do hedge funds exploit rare disaster concerns? *Review of Financial Studies* 31(7), 2650–2692.

Gao, George P., Xiaomeng Lu, and Zhaogang Song, 2019, Tail risk concerns everywhere, *Management Science* 65(7), 3111–3130.

Jiang, George J., and Yisong S. Tian, 2005, The model-free implied volatility and its information content, *Review of Financial Studies* 18(4), 1305–1342.

Jiang, George J., and Yisong S. Tian, 2007, Extracting model-free volatility from option prices: An examination of the VIX index, *Journal of Derivatives* 14(3), 35–60.

Liu, Mengxi Maggie, Kam Fong Chan, and Robert Faff, 2022, What can we learn from firm-level jump-induced tail risk around earnings announcements? *Journal of Banking & Finance* 138, 106409.

Neumann, Michael, and George Skiadopoulos, 2013, Predictable dynamics in higher-order risk-neutral moments: Evidence from the S&P 500 options, *Journal of Financial and Quantitative Analysis* 48(3), 947–977.

Ruan, Xinfeng, and Jin E. Zhang, 2018, Risk-neutral moments in the crude oil market, *Energy Economics* 72, 583–600.

Stilger, Przemysław S., Alexandros Kostakis, and Ser-Huang Poon, 2017, What does risk-neutral skewness tell us about future stock returns? *Management Science* 63(6), 1814–1834.

Zhang, Jin E., and Yi Xiang, 2008, The implied volatility smirk, *Quantitative Finance* 8(3), 263–284.

Appendix

A Derivations of the Model-Free Measure of the RIX

On the basis of Equation (8), both Equations (2) and (7) can be regarded as $H(x)$. Then, the application process on the RIX is as follows

$$\begin{aligned} H(x) &= 6\left(\frac{x}{F_t^T} - 1 - \ln\frac{x}{F_t^T} - \frac{1}{2}\ln^2\frac{x}{F_t^T}\right), \\ H_x(x) &= 6\left(\frac{1}{F_t^T} - \frac{1}{x} - \frac{1}{x}\ln\frac{x}{F_t^T}\right), \\ H_{xx}(x) &= \frac{6}{x^2}\ln\frac{x}{F_t^T}. \end{aligned} \tag{A.1}$$

Therefore, the model-free measure of the RIX at time t is

$$\begin{aligned} RIX_t =& E_t^{\mathbb{Q}}\Bigg[6\left(\frac{F_t^T}{F_t^T} - 1 - \ln\frac{F_t^T}{F_t^T} - \frac{1}{2}\ln^2\frac{F_t^T}{F_t^T}\right) + 6\left(\frac{1}{F_t^T} - \frac{1}{F_t^T} - \frac{1}{F_t^T}\ln\frac{F_t^T}{F_t^T}\right)\left(x - F_t^T\right) \\ &+ \int_0^{F_t^T}\frac{6}{K^2}\ln\frac{K}{F_t^T}P_T(K)\,dK + \int_{F_t^T}^{\infty}\frac{6}{K^2}\ln\frac{K}{F_t^T}C_T(K)\,dK\Bigg] \\ =& e^{r\tau}\left[\int_0^{F_t^T}\frac{6}{K^2}\ln\frac{K}{F_t^T}P_t(K)\,dK + \int_{F_t^T}^{\infty}\frac{6}{K^2}\ln\frac{K}{F_t^T}C_t(K)\,dK\right]. \end{aligned} \tag{A.2}$$

Similarly, TM is

$$\begin{aligned} H(x) &= \ln^3\frac{x}{F_t^T}, \\ H_x(x) &= \frac{3}{x}\ln^2\frac{x}{F_t^T}, \\ H_{xx}(x) &= \frac{6}{x^2}\ln\frac{x}{F_t^T} - \frac{3}{x^2}\ln^2\frac{x}{F_t^T}. \end{aligned} \tag{A.3}$$

Thus, the model-free measure of the TM at time t is

$$\begin{aligned} TM_t =& E_t^{\mathbb{Q}}\Bigg[\ln^3\frac{F_t^T}{F_t^T} + \frac{3}{F_t^T}\ln^2\frac{F_t^T}{F_t^T}\left(x - F_t^T\right) + \int_0^{F_t^T}\left(\frac{6}{K^2}\ln\frac{K}{F_t^T} - \frac{3}{K^2}\ln^2\frac{K}{F_t^T}\right)P_T(K)\,dK \\ &+ \int_{F_t^T}^{\infty}\left(\frac{6}{K^2}\ln\frac{K}{F_t^T} - \frac{3}{K^2}\ln^2\frac{K}{F_t^T}\right)C_T(K)\,dK\Bigg] \\ =& e^{r\tau}\left[\int_0^{F_t^T}\left(\frac{6}{K^2}\ln\frac{K}{F_t^T} - \frac{3}{K^2}\ln^2\frac{K}{F_t^T}\right)P_t(K)\,dK + \int_{F_t^T}^{\infty}\left(\frac{6}{K^2}\ln\frac{K}{F_t^T} - \frac{3}{K^2}\ln^2\frac{K}{F_t^T}\right)C_t(K)\,dK\right]. \end{aligned} \tag{A.4}$$

B Derivations of the RIX Under the Gram-Charlier Density

Under the Gram-Charlier density, the values of three components of Equation (2) are as follows:

$$
\begin{aligned}
E_t^{\mathbb{Q}}\left(\frac{S_T}{F_t^T}-1\right) &= 0,\\
\mathbb{IV} &= E_t^{\mathbb{Q}}\left(-\ln\frac{S_T}{F_t^T}\right)\\
&= -E_t^{\mathbb{Q}}\left(\ln\frac{S_T}{F_t^T}\right)\\
&= -E_t^{\mathbb{Q}}\left[\left(-\frac{1}{2}\sigma^2+\mu_c\right)\tau+\sigma\sqrt{\tau}y\right]\\
&= \frac{1}{2}\sigma^2\tau-\mu_c\tau-\sigma\sqrt{\tau}E_t^{\mathbb{Q}}\left(y\right)\\
&= \frac{1}{2}\sigma^2\tau-\mu_c\tau,\\
\mathbb{V} &= E_t^{\mathbb{Q}}\left(-\frac{1}{2}\ln^2\frac{S_T}{F_t^T}\right)\\
&= -\frac{1}{2}\left[\left(-\frac{1}{2}\sigma^2+\mu_c\right)\tau\right]^2-\frac{1}{2}\left[\left(\sigma\sqrt{\tau}\right)^2E_t^{\mathbb{Q}}\left(y^2\right)\right]\\
&= -\frac{1}{2}\left(-\frac{1}{2}\sigma^2+\mu_c\right)^2\tau^2-\frac{1}{2}\sigma^2\tau.
\end{aligned}
\tag{B.1}
$$

Therefore, the RIX of full range under Gram-Charlier Density is the combination of these values times 6, which is shown as Equation (14).

C Derivations of the TM Under the Gram-Charlier Density

Under the Gram-Charlier density, Equation (7) can be written as:

$$
\begin{aligned}
E_t^{\mathbb{Q}}\left(\ln^3\frac{S_T}{F_t^T}\right) =& E_t^{\mathbb{Q}}\left\{\left[\left(-\frac{1}{2}\sigma^2+\mu_c\right)\tau+\sigma\sqrt{\tau}y\right]^3\right\}\\
=& \left(-\frac{1}{2}\sigma^2+\mu_c\right)^3\tau^3+3\left[\left(-\frac{1}{2}\sigma^2+\mu_c\right)\tau\right]^2\sigma\sqrt{\tau}E_t^{\mathbb{Q}}\left(y\right)\\
&+3\left(-\frac{1}{2}\sigma^2+\mu_c\right)\left(\sigma\tau\right)^2E_t^{\mathbb{Q}}\left(y^2\right)+\left(\sigma\sqrt{\tau}\right)^3E_t^{\mathbb{Q}}\left(y^3\right)\\
=& \left(-\frac{1}{2}\sigma^2+\mu_c\right)^3\tau^3+3\left(-\frac{1}{2}\sigma^2+\mu_c\right)\left(\sigma\tau\right)^2+\left(\sigma\sqrt{\tau}\right)^3\lambda_1,
\end{aligned}
\tag{C.1}
$$

which is Equation (16).

D Derivations of the RIX^{-} Under the Gram-Charlier Density

Under the Gram-Charlier density, β_0, β_1, and β_2 can be considered as semi-probability, semi-expectation of y, and semi-second moment of y:

$$
\begin{aligned}
\beta_0 =& E_t^{\mathbb{Q}}\left(\mathbb{1}_{S_T<F_t^T}\right)\\
=& \int_{-\infty}^{-d_2} f(y)\,dy\\
=& \int_{-\infty}^{-d_2} \left[n(y) - \frac{\lambda_1}{3!}\frac{d^3 n(y)}{dy^3} + \frac{\lambda_2}{4!}\frac{d^4 n(y)}{dy^4}\right] dy\\
=& \int_{-\infty}^{-d_2} n(y)\,dy - \frac{\lambda_1}{3!}\int_{-\infty}^{-d_2}(-y^3+3y)n(y)\,dy + \frac{\lambda_2}{4!}\int_{-\infty}^{-d_2}(y^4-6y^2+3)n(y)\,dy\\
=& N(-d_2) + \frac{\lambda_1}{3!}[-d_2^2 n(-d_2) - 2n(-d_2) + 3n(-d_2)]\\
&+ \frac{\lambda_2}{4!}[d_2^3 n(-d_2) + 3d_2 n(-d_2) + 3N(-d_2) - 6d_2 n(-d_2) - 6N(-d_2) + 3N(-d_2)]\\
=& N(-d_2) + \frac{\lambda_1}{3!}(-d_2^2+1)n(-d_2) + \frac{\lambda_2}{4!}(d_2^3 - 3d_2)n(-d_2),\\
\beta_1 =& E_t^{\mathbb{Q}}\left(y \times \mathbb{1}_{S_T<F_t^T}\right)\\
=& \int_{-\infty}^{-d_2} y f(y)\,dy\\
=& \int_{-\infty}^{-d_2} y n(y)\,dy - \frac{\lambda_1}{3!}\int_{-\infty}^{-d_2}(-y^4+3y^2)n(y)\,dy + \frac{\lambda_2}{4!}\int_{-\infty}^{-d_2}(y^5-6y^3+3y)n(y)\,dy\\
=& -n(-d_2) + \frac{\lambda_1}{3!}[d_2^3 n(-d_2) + 3d_2 n(-d_2) + 3N(-d_2) - 3d_2 n(-d_2) - 3N(-d_2)]\\
&+ \frac{\lambda_2}{4!}[-d_2^4 n(-d_2) - 4d_2^2 n(-d_2) - 8n(-d_2) + 6d_2^2 n(-d_2) + 12n(-d_2) - 3n(-d_2)]\\
=& -n(-d_2) + \frac{\lambda_1}{3!}d_2^3 n(-d_2) + \frac{\lambda_2}{4!}(-d_2^4 + 2d_2^2 + 1)n(-d_2),\\
\beta_2 =& E_t^{\mathbb{Q}}\left(y^2 \times \mathbb{1}_{S_T<F_t^T}\right)^2\\
=& \int_{-\infty}^{-d_2} y^2 f(y)\,dy\\
=& \int_{-\infty}^{-d_2} y^2 n(y)\,dy - \frac{\lambda_1}{3!}\int_{-\infty}^{-d_2}(-y^5+3y^3)n(y)\,dy + \frac{\lambda_2}{4!}\int_{-\infty}^{-d_2}(y^6-6y^4+3y^2)n(y)\,dy\\
=& d_2 n(-d_2) + N(-d_2) + \frac{\lambda_1}{3!}[-d_2^4 n(-d_2) - 4d_2^2 n(-d_2) - 8n(-d_2) + 3d_2^2 n(-d_2)\\
&+ 6n(-d_2)] + \frac{\lambda_2}{4!}[d_2^5 n(-d_2) + 5d_2^3 n(-d_2) + 15d_2 n(-d_2) + 15N(-d_2) - 6d_2^3 n(-d_2)\\
&- 18d_2 n(-d_2) - 18N(-d_2) + 3d_2 n(-d_2) + 3N(-d_2)]\\
=& d_2 n(-d_2) + N(-d_2) + \frac{\lambda_1}{3!}(-d_2^4 - d_2^2 - 2)n(-d_2) + \frac{\lambda_2}{4!}(d_2^5 - d_2^3)n(-d_2).
\end{aligned}
\tag{D.1}
$$

$$\begin{aligned}
E_t^{\mathbb{Q}}\left(\ln\frac{S_T}{F_t^T}\times \mathbb{1}_{S_T<F_t^T}\right) &= E_t^{\mathbb{Q}}\left\{\left[\left(-\frac{1}{2}\sigma^2+\mu_c\right)\tau+\sigma\sqrt{\tau}y\right]\times \mathbb{1}_{S_T<F_t^T}\right\} \\
&= \left(-\frac{1}{2}\sigma^2+\mu_c\right)\tau\beta_0+\sigma\sqrt{\tau}\beta_1, \\
E_t^{\mathbb{Q}}\left[\frac{1}{2}\left(\ln^2\frac{S_T}{F_t^T}\times \mathbb{1}_{S_T<F_t^T}\right)\right] &= \frac{1}{2}E_t^{\mathbb{Q}}\left\{\left[\left(-\frac{1}{2}\sigma^2+\mu_c\right)\tau+\sigma\sqrt{\tau}y\right]^2\times \mathbb{1}_{S_T<F_t^T}\right\} \\
&= \frac{1}{2}E_t^{\mathbb{Q}}\left\{\left[\left(-\frac{1}{2}\sigma^2+\mu_c\right)^2\tau^2+2\left(-\frac{1}{2}\sigma^2+\mu_c\right)\sigma\tau^{\frac{3}{2}}y+\sigma^2\tau y^2\right]\times \mathbb{1}_{S_T<F_t^T}\right\} \\
&= \frac{1}{2}\left(-\frac{1}{2}\sigma^2+\mu_c\right)^2\tau^2\beta_0+\left(-\frac{1}{2}\sigma^2+\mu_c\right)\sigma\left(\sqrt{\tau}\right)^3\beta_1+\frac{1}{2}\sigma^2\tau\beta_2.
\end{aligned} \tag{D.2}$$

Then, B, C, and D can be obtained by regrouping the coefficients of β_0, β_1, and β_2, respectively.

E Derivations of the TM^- Under the Gram-Charlier Density

Under the Gram-Charlier density, β_3 can be considered as the semi-third moment of y:

$$\begin{aligned}
\beta_3 =& E_t^{\mathbb{Q}}\left(y^3\times \mathbb{1}_{S_T<F_t^T}\right) \\
=& \int_{-\infty}^{-d_2} y^3 f(y)\,dy \\
=& \int_{-\infty}^{-d_2} y^3 n(y)\,dy - \frac{\lambda_1}{3!}\int_{-\infty}^{-d_2}(-y^6+3y^4)n(y)\,dy + \frac{\lambda_2}{4!}\int_{-\infty}^{-d_2}(y^7-6y^5+3y^3)n(y)\,dy \\
=& -d_2^2 n(-d_2) + -2n(-d_2) \\
&+ \frac{\lambda_1}{3!}[d_2^5 n(-d_2)+5d_2^3 n(-d_2)+15d_2 n(-d_2)+15N(-d_2)-3d_2^3 n(-d_2)-9d_2 n(-d_2)-9N(-d_2)] \\
&+ \frac{\lambda_2}{4!}[-d_2^6 n(-d_2)-3d_2^2 n(-d_2)-6n(-d_2)] \\
=& (-d_2^2-2)n(-d_2)+\frac{\lambda_1}{3!}[(d_2^5+2d_2^3+6d_2)n(-d_2)+6N(-d_2)]+\frac{\lambda_2}{4!}(-d_2^6-3d_2^2-6)n(-d_2).
\end{aligned} \tag{E.1}$$

In addition, G, H, I, and J can be obtained by expanding the semi-third moment under the Gram-Charlier density and regrouping the coefficients of β_0, β_1, β_2, and β_3, respectively.

Figures

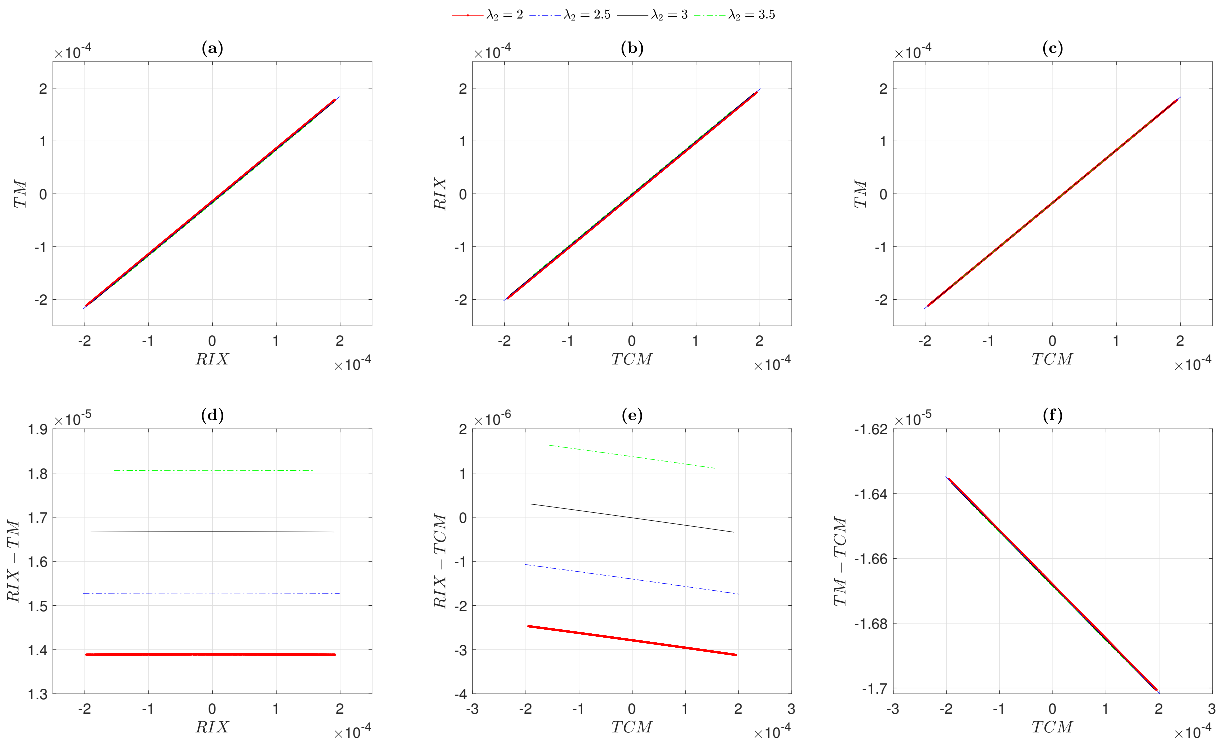

Figure 1: Relationships among the RIX, TM and TCM.
This figure shows the relationships among the RIX, TM and TCM, with the setting of $\sigma = 0.2$, $\tau = 1/12$, and $\lambda_2 = 2, 2.5, 3,$ and 3.5, based on Equation (14) and Equation (16).

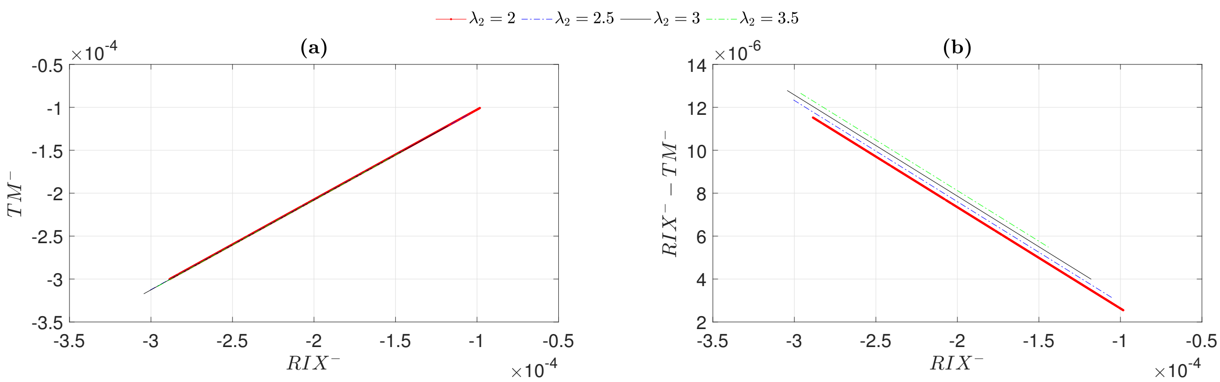

Figure 2: Relationship between the RIX^- and TM^-.
This figure shows the relationship between the RIX^- and TM^-, with the setting of $\sigma = 0.2$, $\tau = 1/12$, and $\lambda_2 = 2, 2.5, 3,$ and 3.5, based on Equation (20) and Equation (22).

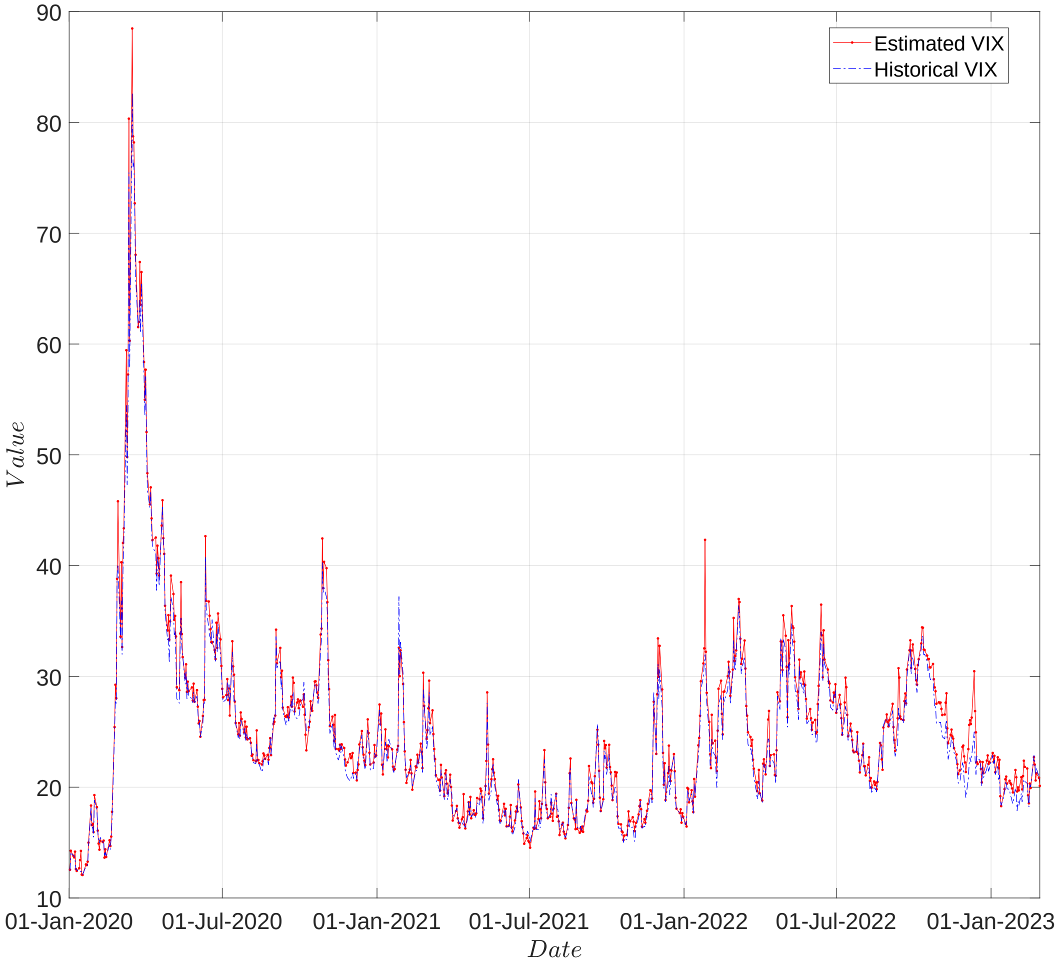

Figure 3: Comparison between the CBOE VIX and the Estimated VIX. This figure shows the comparison between the CBOE VIX and the Estimated VIX, with linear interpolation and constant extrapolation of the implied volatility curve and setting $\Delta K = 0.05\% \times F_t^T$ and $a = 0.25$, based on Equation (35), from 1 January, 2020 to 28 February, 2023. The correlation is 0.99.

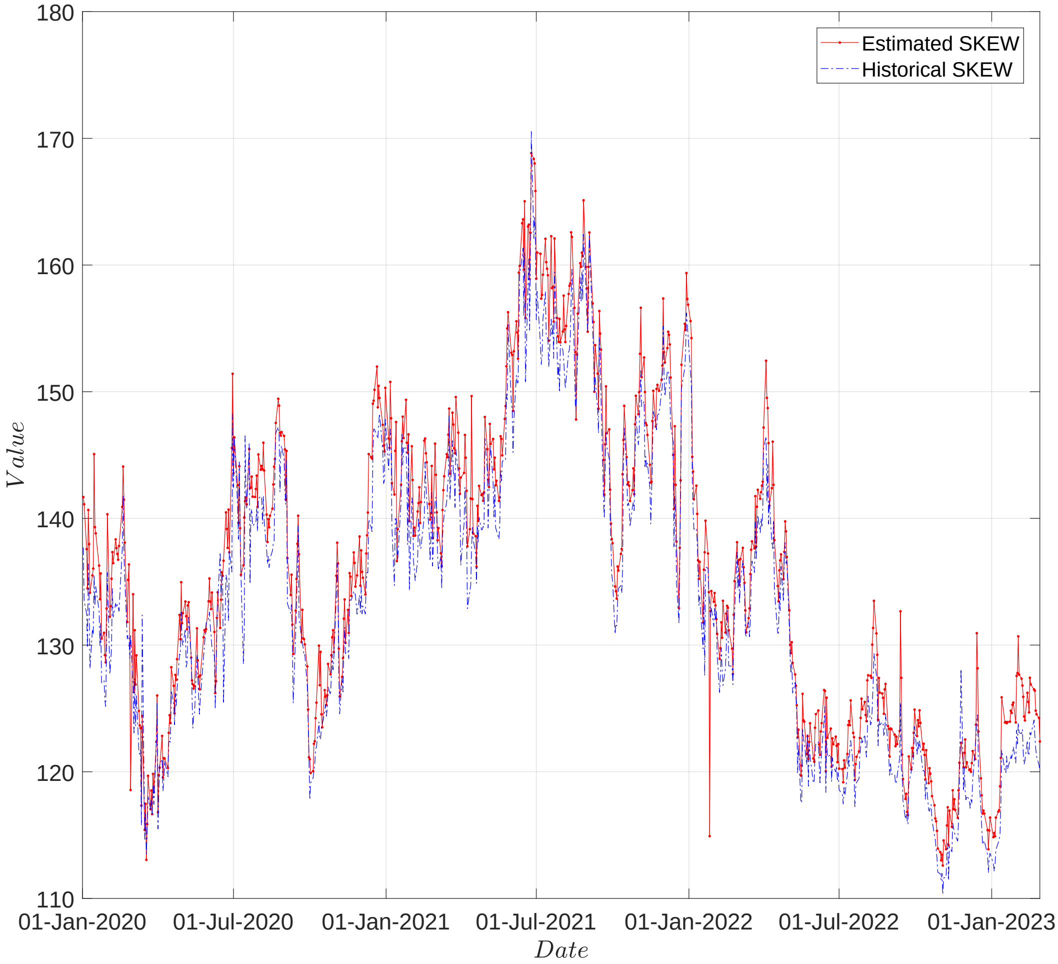

Figure 4: Comparison between the CBOE $SKEW$ and the Estimated $SKEW$. This figure shows the comparison between the CBOE $SKEW$ and the Estimated $SKEW$, with linear interpolation and constant extrapolation of the implied volatility curve and setting $\Delta K = 0.05\% \times F_t^T$ and $a = 0.25$, based on Equation (36), from 1 January, 2020 to 28 February, 2023. The correlation is 0.97.

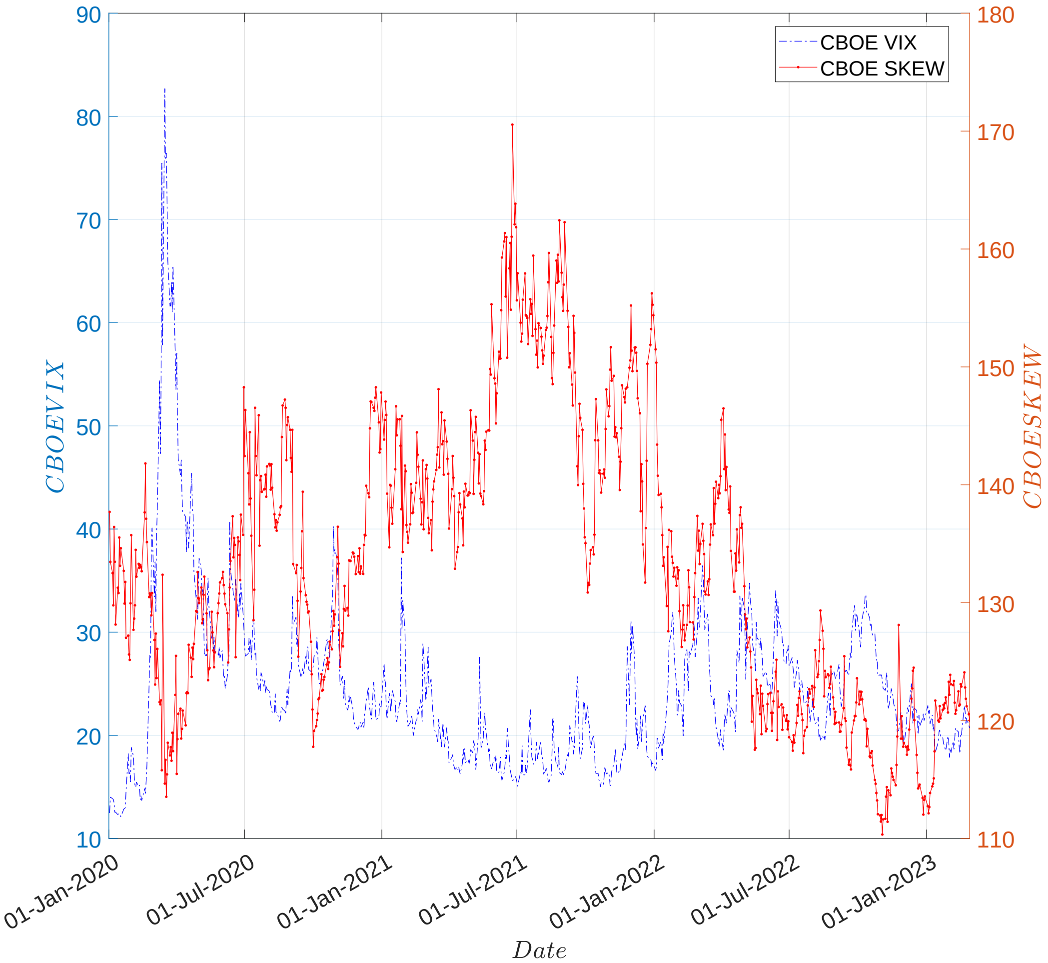

Figure 5: Comparison between the trend of the VIX and $SKEW$.
This figure shows the comparison between the trend of the VIX and $SKEW$ from 1 January 2020, to 28 February, 2023.

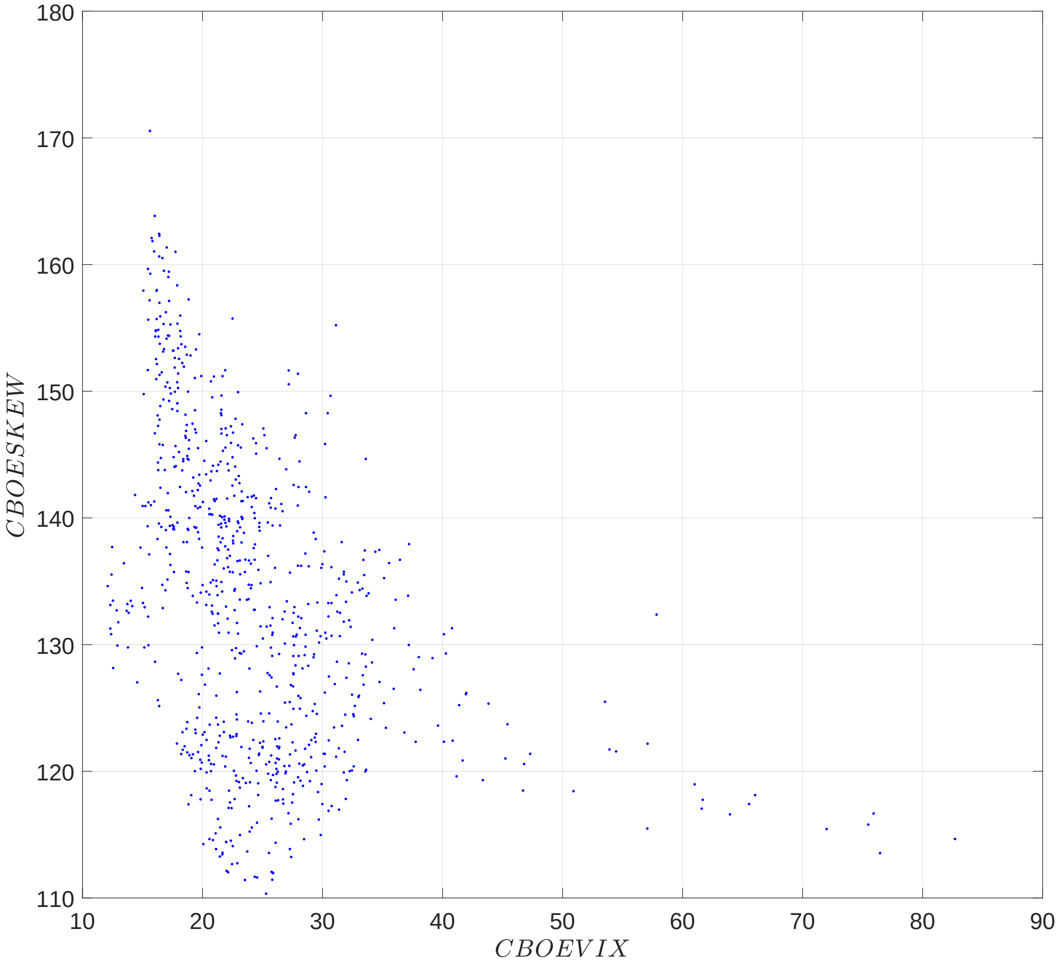

Figure 6: Scatter plot of the VIX and $SKEW$.
This figure is a scatter plot of the VIX and $SKEW$ from 1 January, 2020 to 28 February, 2023.

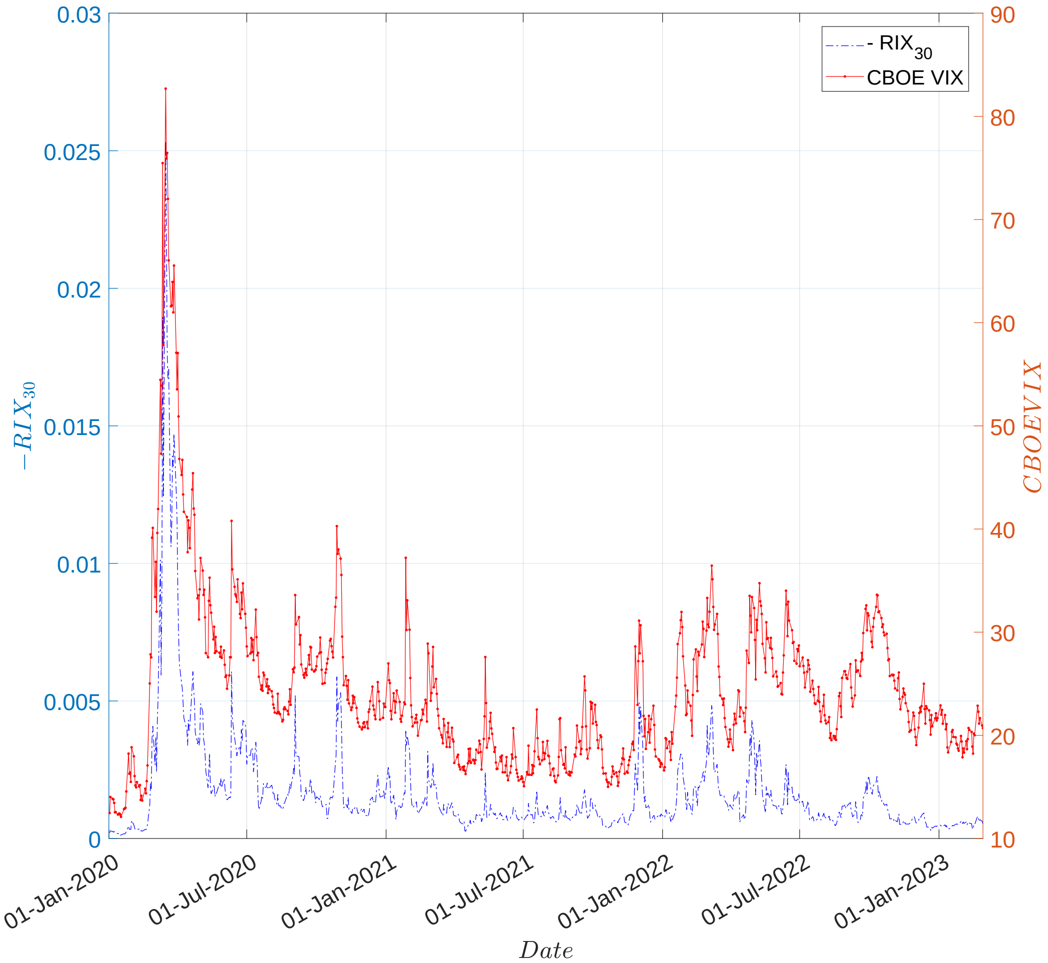

Figure 7: Comparison between the trend of VIX and $-RIX_{30}$.
This figure shows the comparison between the trend of VIX and $-RIX_{30}$ from 1 January 2020 to 28 February 2023.

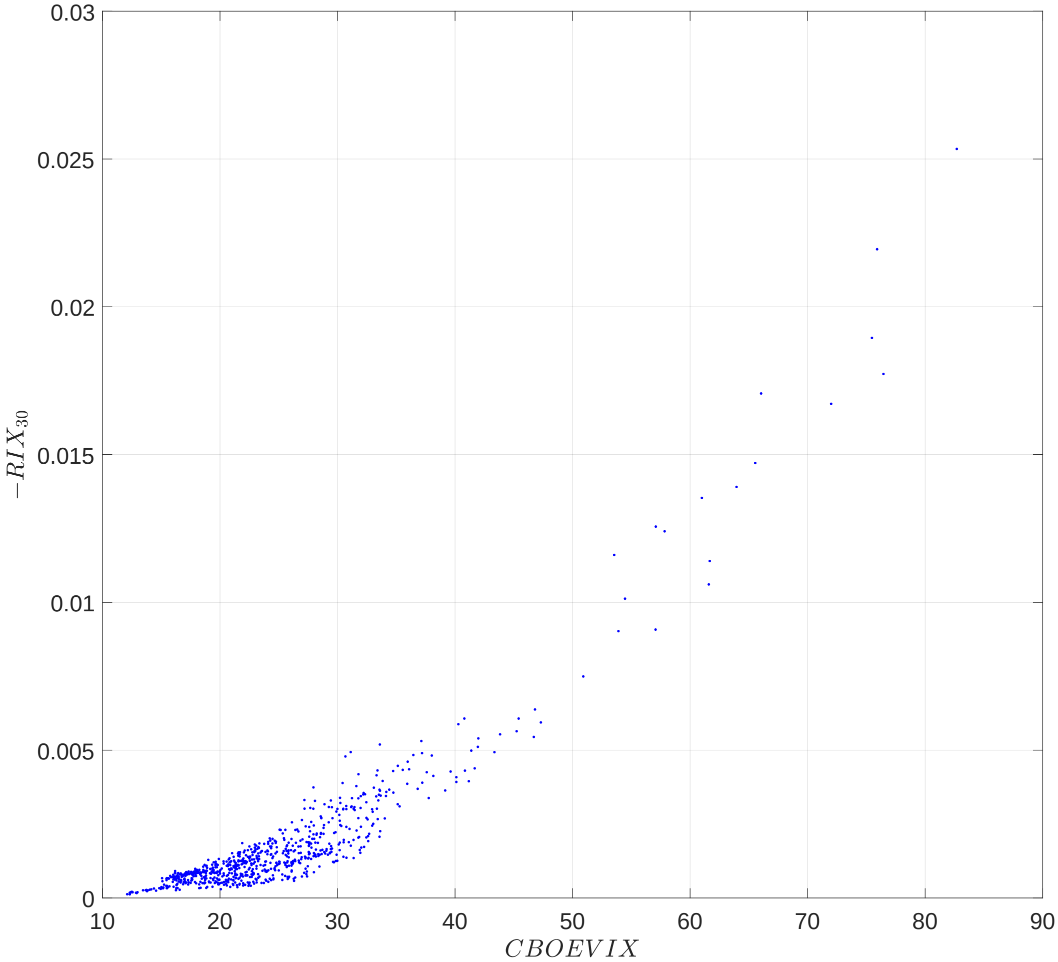

Figure 8: Scatter plot of VIX and $-RIX_{30}$.
This figure is a scatter plot of VIX and $-RIX_{30}$ from 1 January 2020 to 28 February 2023.

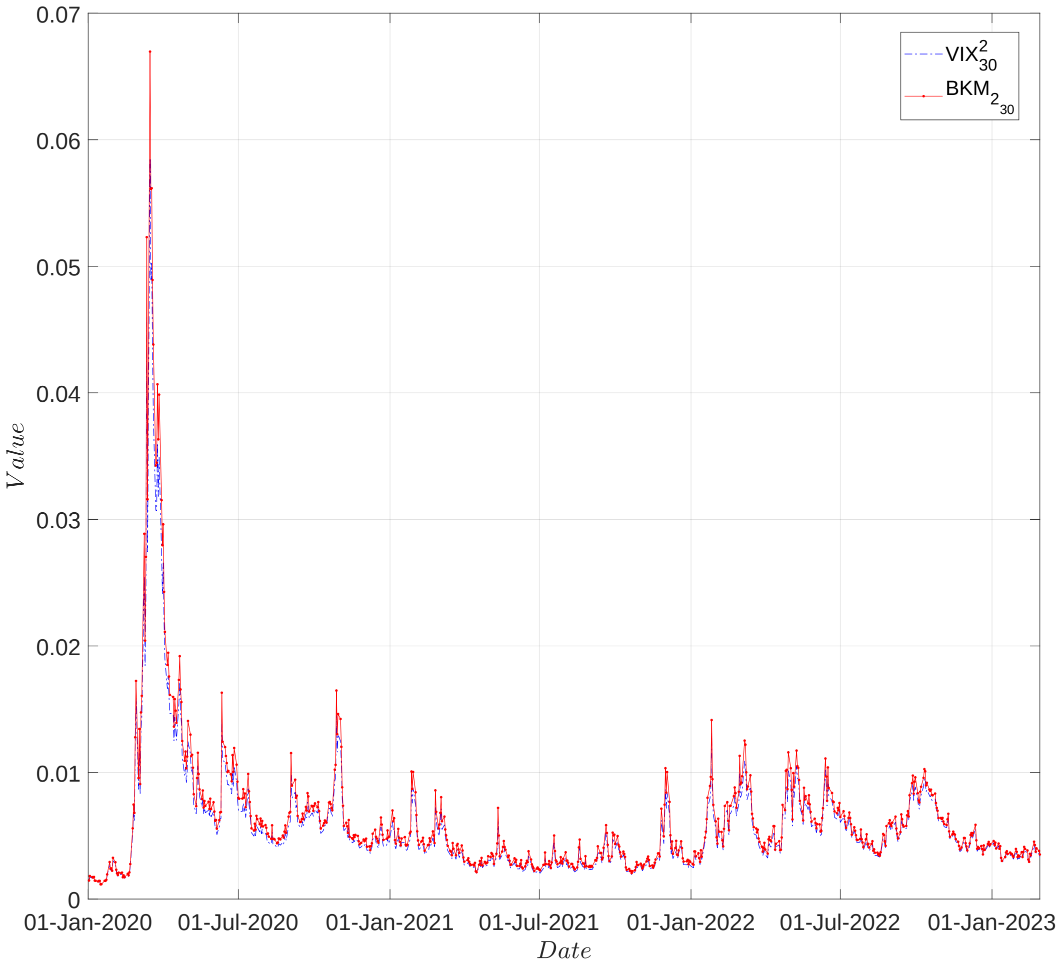

Figure 9: Comparison between the trend of the $BKM_{2_{30}}$ and VIX^2_{30}.
This figure shows the comparison between the trend of the BKM_2 and VIX^2 with a 30-day term structure from 1 January, 2020 to 28 February, 2023.

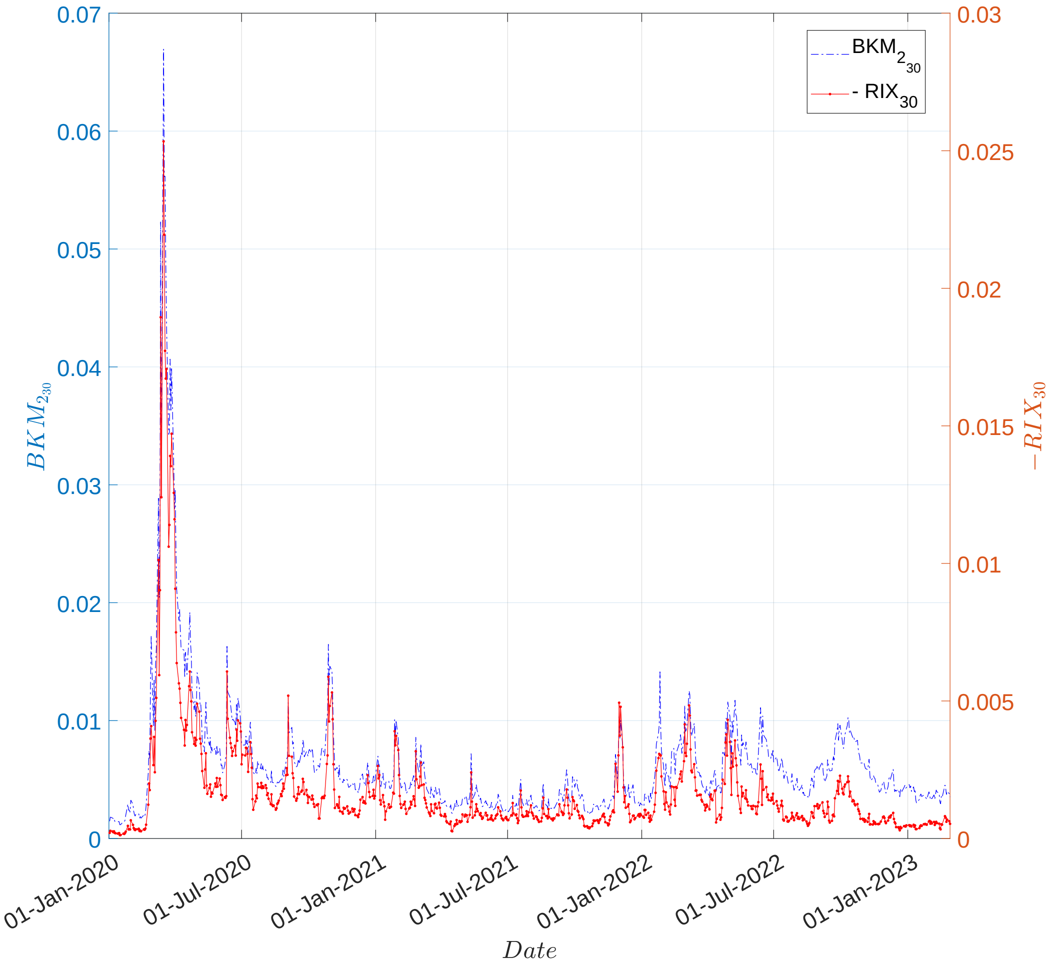

Figure 10: Comparison between the trend of the $BKM_{2_{30}}$ and $-RIX_{30}$.
This figure shows the comparison between the trend of the BKM_2 and $-RIX$ with a 30-day term structure from 1 January, 2020 to 28 February, 2023.

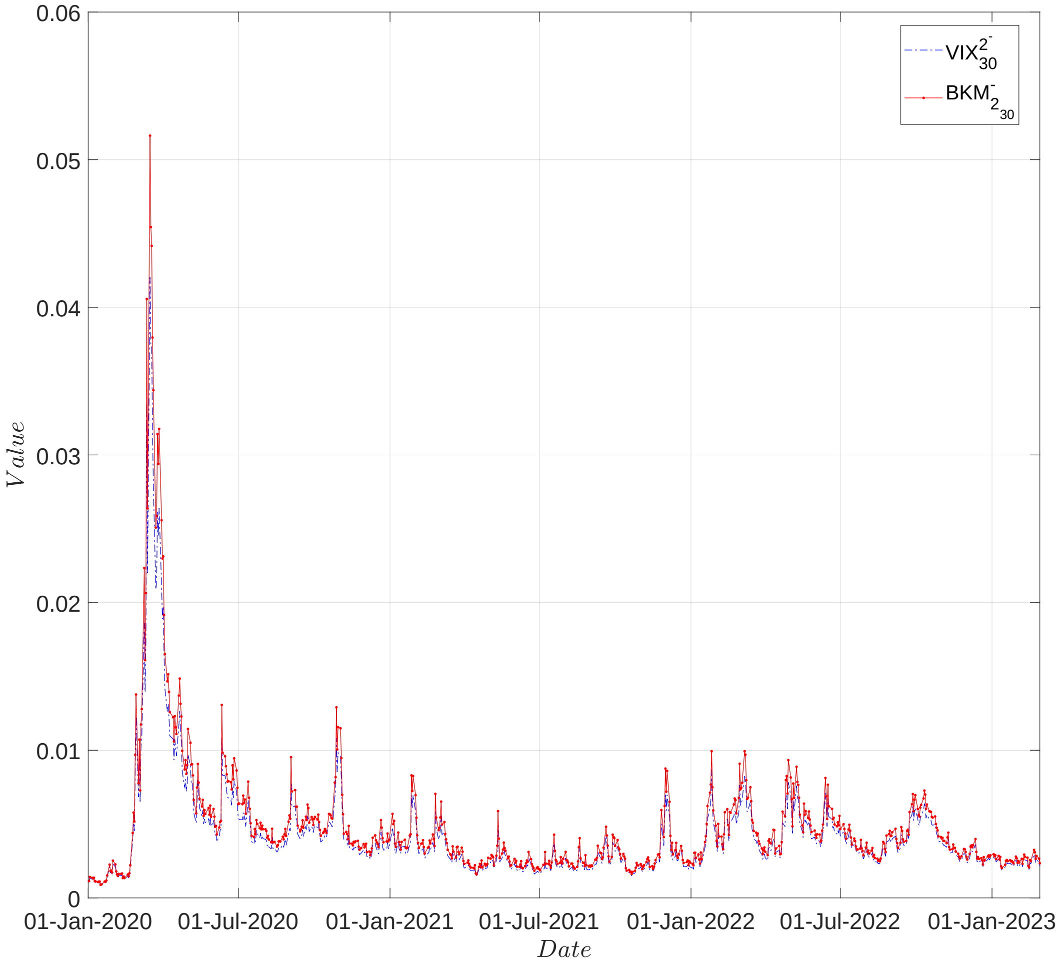

Figure 11: Comparison between the trend of the $BKM_{2_{30}}$ an VIX^{2-}_{30}.
This figure shows the comparison between the trend of the BKM_2^- and VIX^{2-} with a 30-day term structure from 1 January, 2020 to 28 February, 2023.

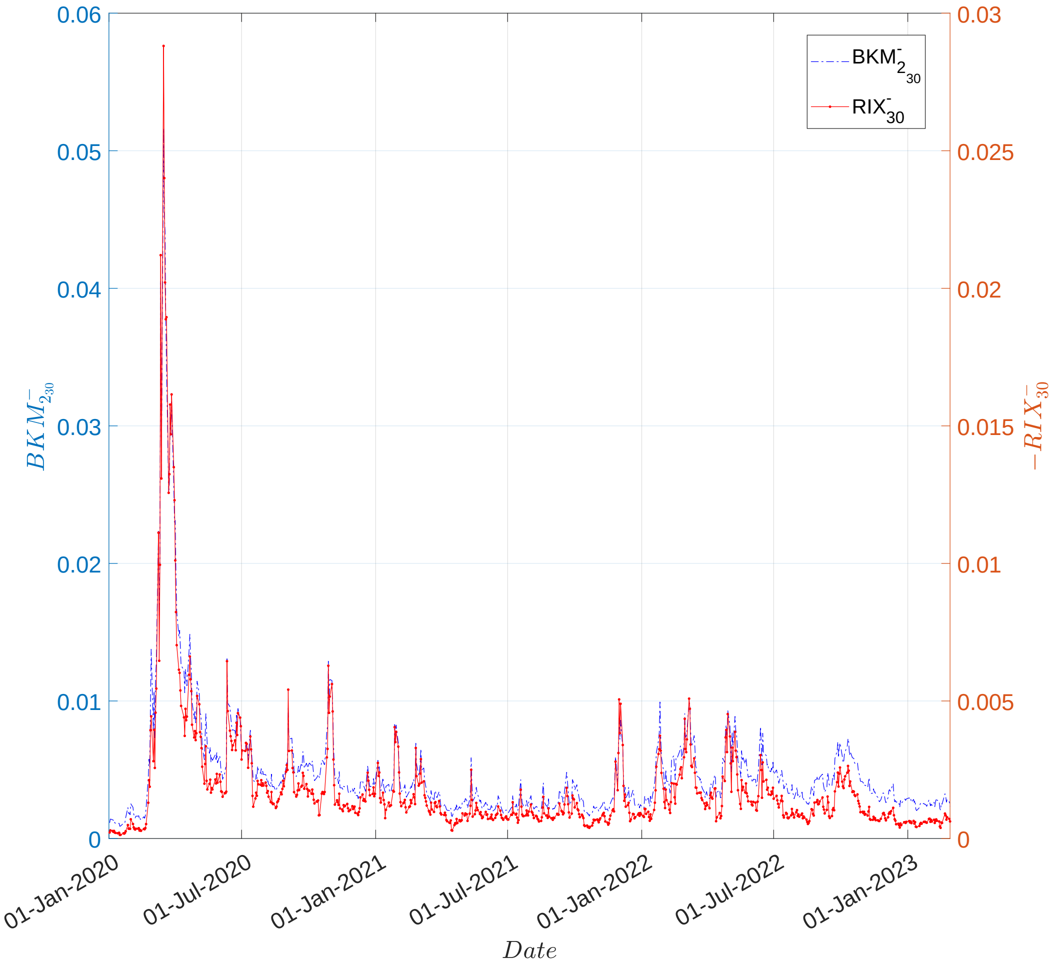

Figure 12: Comparison between the trend of the $BKM^-_{2_{30}}$ and $-RIX^-_{30}$. This figure shows the comparison between the trend of the BKM^-_2 and $-RIX^-$ with a 30-day term structure from 1 January, 2020 to 28 February, 2023.

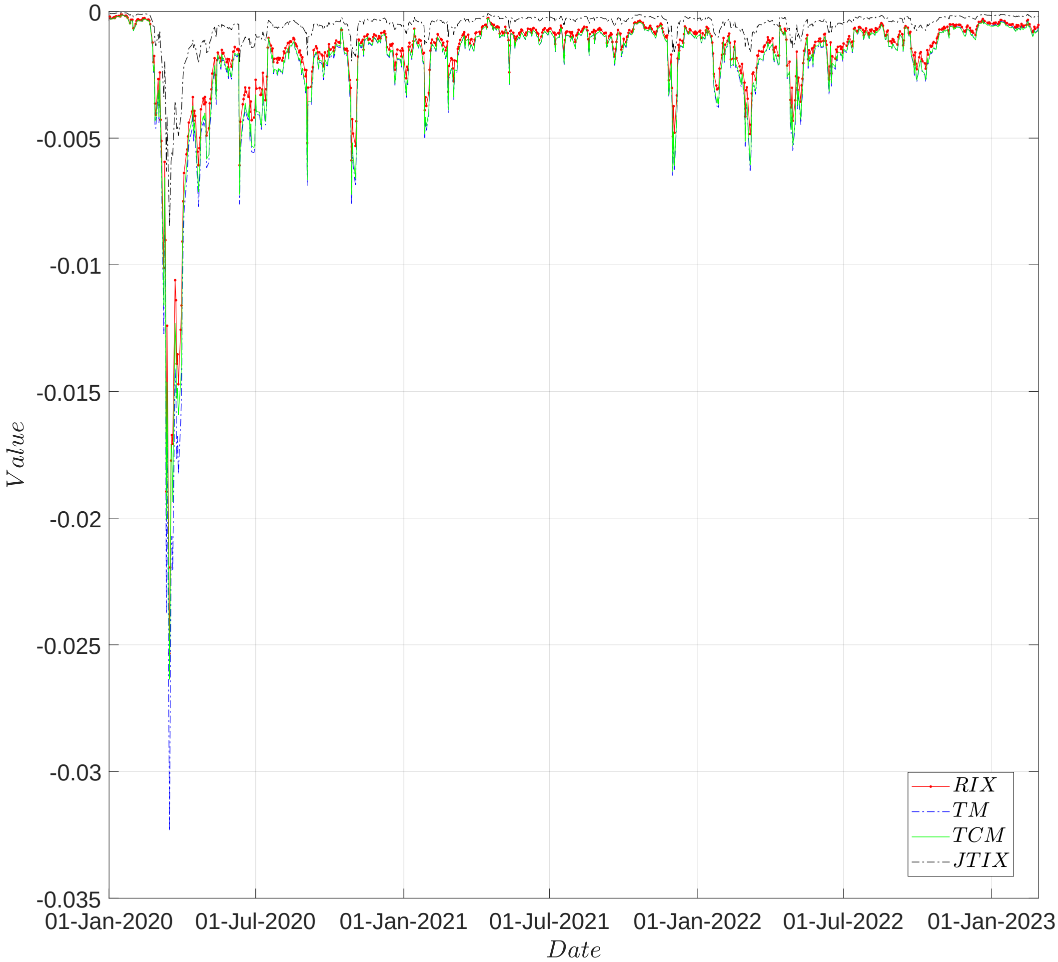

Figure 13: Comparison among the trends of the RIX_{30}, $-JTIX_{30}$, TM_{30}, and TCM_{30}.

This figure shows the comparison among the trends of the RIX, $-JTIX$, TM, and TCM with a 30-day term structure from 1 January, 2020 to 28 February, 2023.

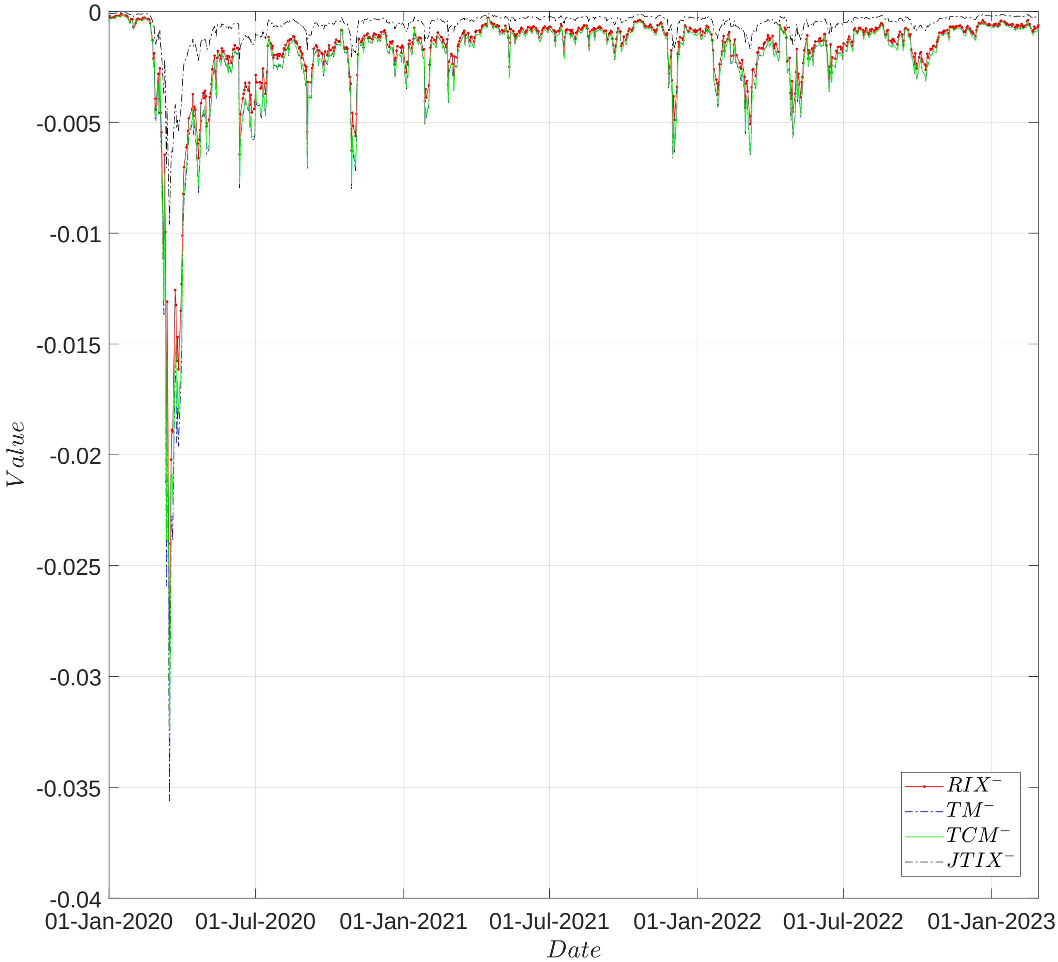

Figure 14: Comparison among the trends of the RIX_{30}^-, $-JTIX_{30}^-$, TM_{30}^-, and TCM_{30}^-.

This figure shows the comparison among the trends of the RIX^-, $-JTIX^-$, TM^-, and TCM^- with a 30-day term structure from 1 January, 2020 to 28 February, 2023.

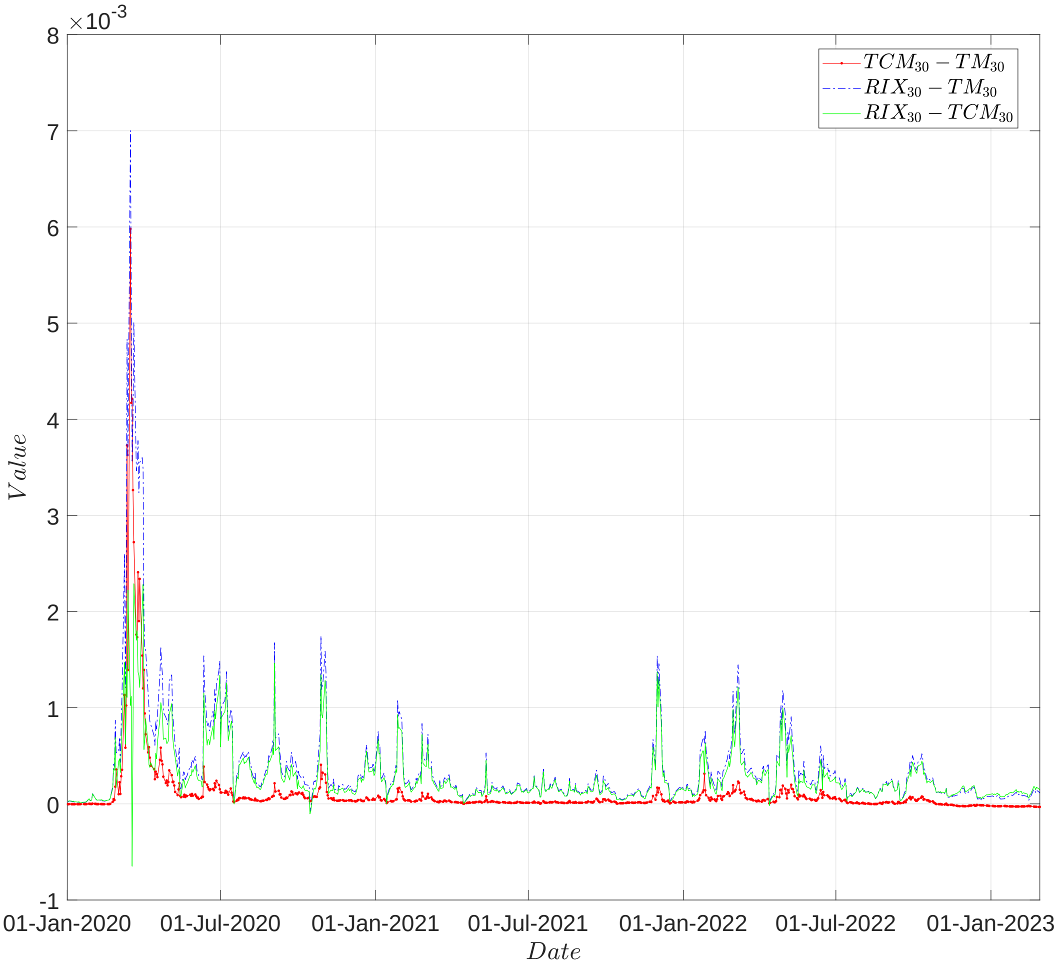

Figure 15: Comparison of the differences among the RIX_{30}, TM_{30}, and TCM_{30}. This figure shows the comparison of the differences among the RIX, TM, and TCM with a 30-day term structure from 1 January, 2020 to 28 February, 2023.

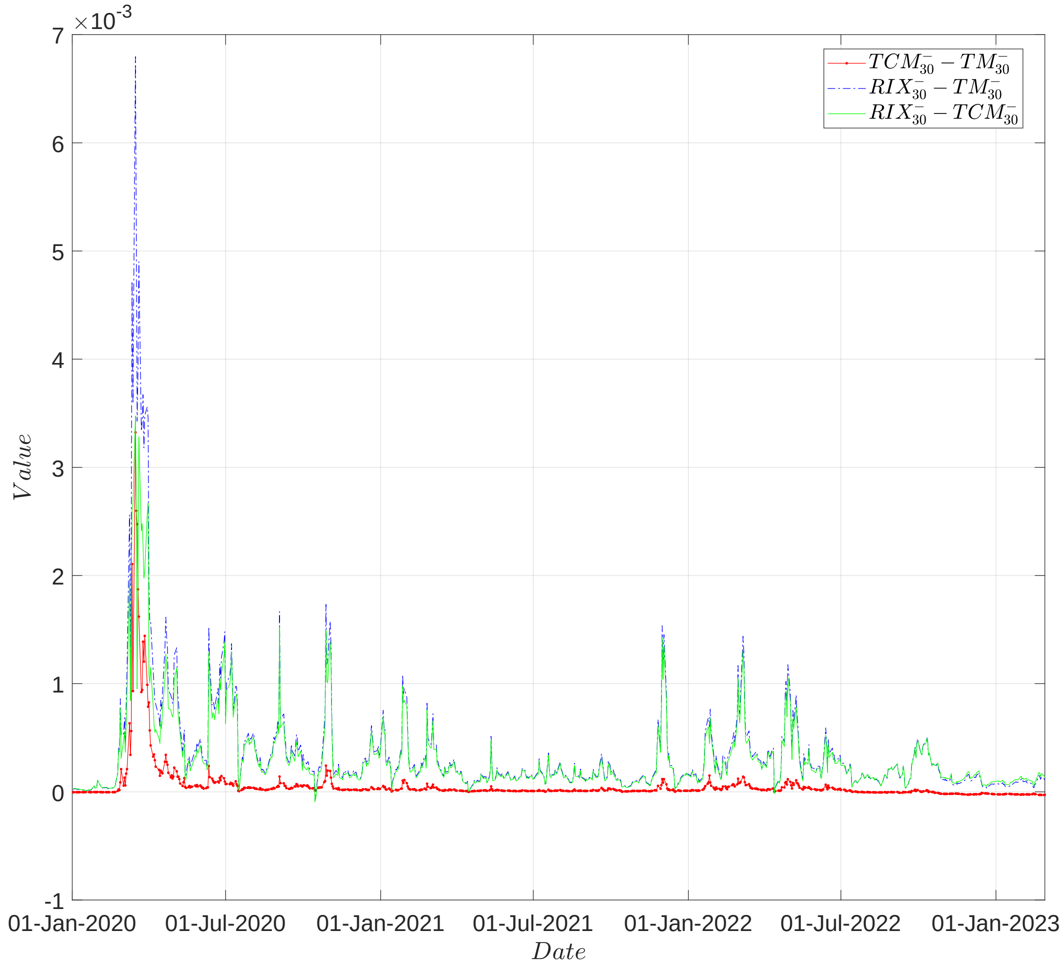

Figure 16: Comparison of the differences among the RIX_{30}, TM_{30}, and TCM_{30}. This figure shows the comparison of the differences among the RIX, TM, and TCM with a 30-day term structure from 1 January, 2020 to 28 February, 2023.

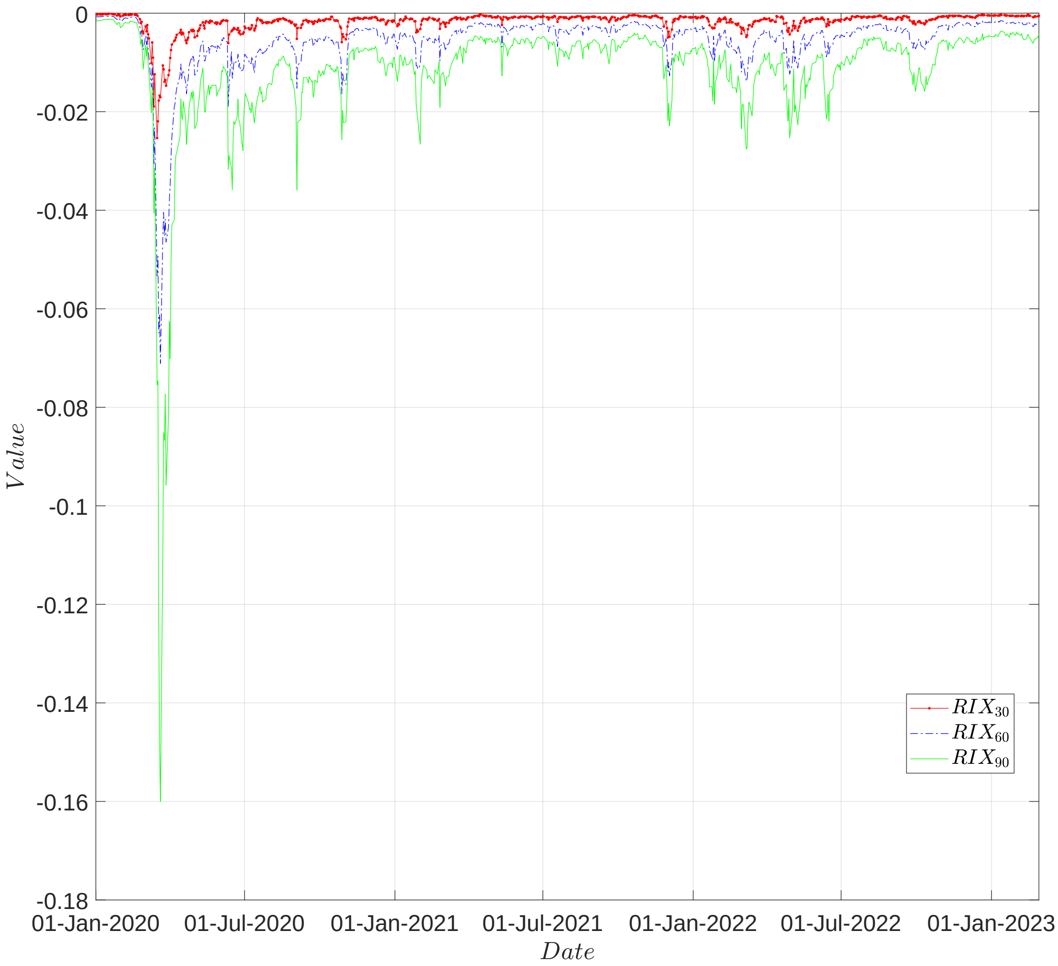

Figure 17: Term structures of the RIX.
This figure shows the term structures of the RIX for 30-day, 60-day, and 90-day periods from 1 January, 2020 to 28 February, 2023.

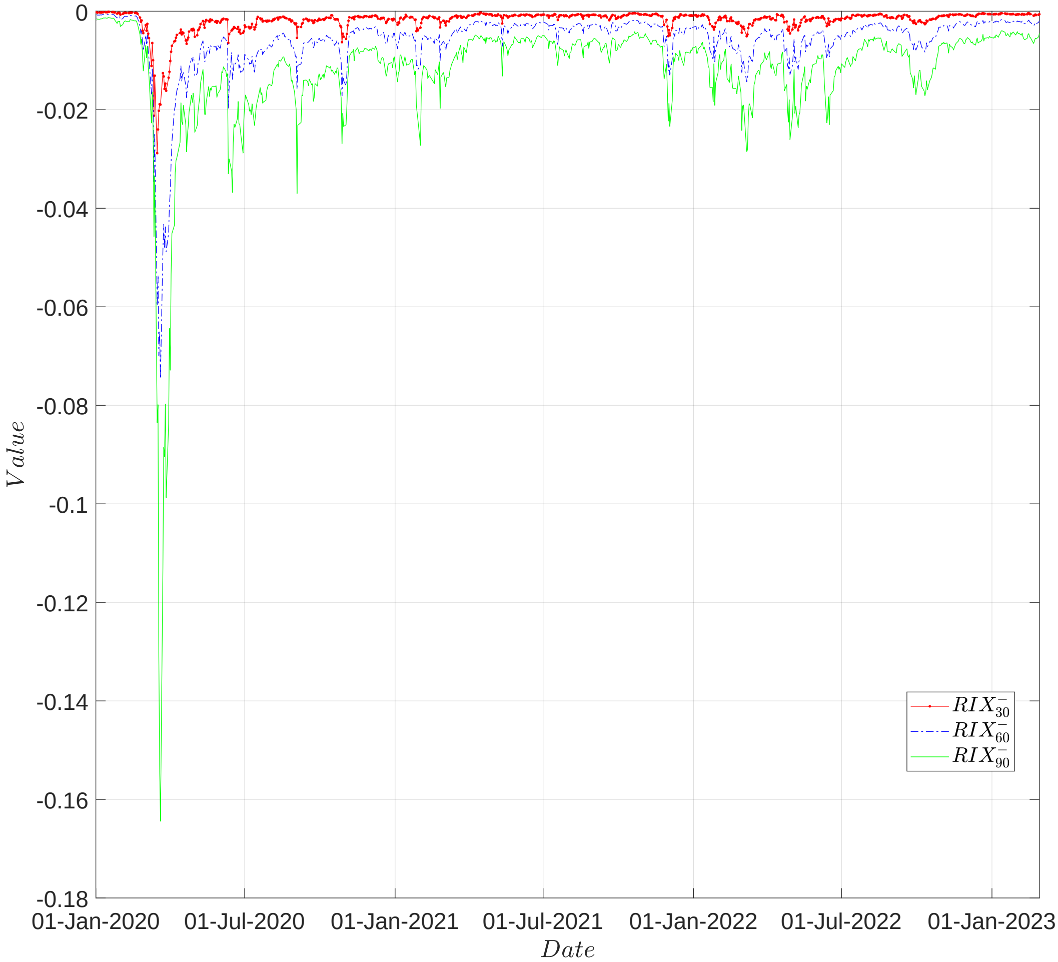

Figure 18: Term structures of the RIX^-.
This figure shows the term structures of the RIX^- for 30-day, 60-day, and 90-day periods from 1 January, 2020 to 28 February, 2023.

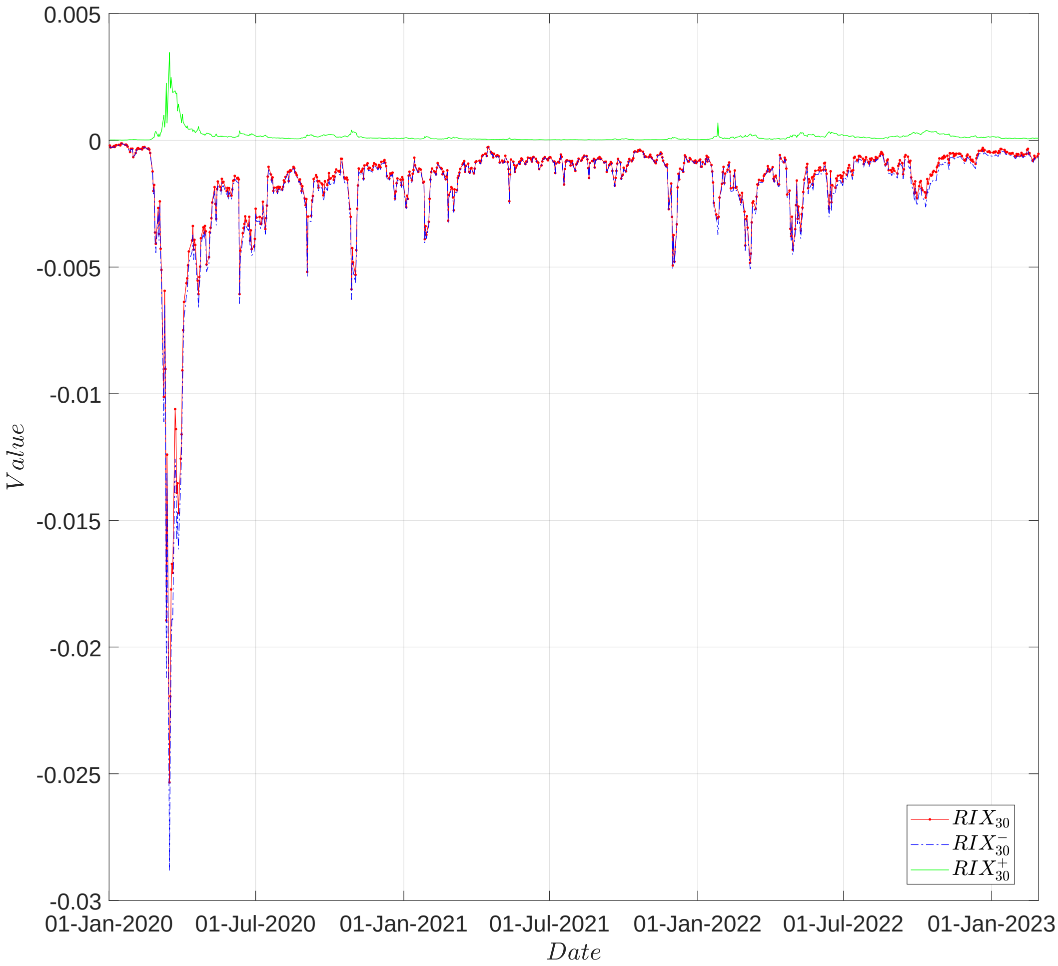

Figure 19: Comparison of different ranges of the RIX_{30}.
This figure shows the comparison of different ranges of the RIX with a 30-day term structure from 1 January, 2020 to 28 February, 2023. The RIX^{+} is calculated from OTM calls based on Equation (23), which is essentially the difference between the RIX and RIX^{-}.